SCIENTIFIC COMMITTEE
NINTH REGULAR SESSION

Pohnpei, Federated States of Micronesia
6-14 August 2013

Project 62: SEAPODYM applications in WCPO

WCPFC-SC9-2012/EB-WP-03 Rev 1

08/08/2013

P.Lehodey[1], I.Senina[1], O.Titaud[1], B.Calmettes[1],

S.Nicol[2], J.Hampton[2], S.Caillot[2], P.Williams[2]

[1] Marine Ecosystem Department, CLS, France.
[2] Oceanic Fisheries Programme, Secretariat of the Pacific Community.

Executive Summary

Recommendation

The SC is advised that the reference fits presented for skipjack, bigeye and south pacific albacore are currently the best available for each species. The biomass estimates however remain above those of MULTIFAN-CL for skipjack and bigeye unless the mortality rates and initial biomass in SEAPODYM are scaled to those estimated by MULTIFAN-CL. For albacore, the last optimization including improvements in both the fisheries definition and the code of the model resulted in a new unconstrained estimate with lower biomass than in the MFCL last assessment. The SC is encouraged to note that the use of finer resolution data has captured more meso-scale variation in tuna distribution which is resulting in the convergence in population estimates between SEAPODYM and MULTIFAN-CL. The SC should also be encouraged by the code developments to incorporate tagging data into the model. The first experiments with this code have resulted in improved estimation of movement parameters and early indications suggest that these data will result in lower biomass estimation and improvement in model fits.

The SC is also advised that the model ensemble approach currently being applied to the construction of physical forcing data to be used in future climate change analyses will allow uncertainties in tuna responses to climate change to be better evaluated.

The SC is requested to note the 2013-2014 work plan for Project 62 which includes the generation of historical reference fits for all species with the inclusion of tagging data, further applications of high resolution data, and new analyses of climate change impacts. The SC is also requested to acknowledge the projects and donors that are continuing to contribute to the development and application of SEAPODYM to the work programme of the WCPFC-SC and requested to endorse the inclusion of all presented projects within the scope of Project 62.

The SC is also invited to note that development of the SEAPODYM model has now progressed to the stage where it can be used to assist the WCPFC and its committees with decisions associated with:

- Developing criteria for the allocation of the total allowable catch or the total level of fishing effort;
- Assessing the impacts of climate variability and change and fishing impacts;
- Marine spatial planning and CMM evaluation; and
- Providing fixed input into MFCL (e.g. recruitment and movement parameters).

The SC is advised to schedule a scientific review of all historical and climate change reference fits (in the agenda of SC10) to facilitate the use of this model in the future work programs of WCPFC and its committees. The review should aim to determine which applications SEAPODYM reference fits are endorsed.

Introduction

SEAPODYM is a model developed for investigating spatial tuna population dynamics, under the influence of both fishing and environmental effects. In addition to fisheries data the model utilises environmental data in a manner that allows high resolution modelling. In this regard the model

complements the Scientific Committee's MULTIFAN-CL models by providing more detailed information on how tuna distributions are structured in space and time. The continued development and application of the SEAPODYM model to the work of the WCPFC Scientific Committee is facilitated through Project 62. The project affiliates the independently funded work on SEAPODYM into the SC's work programme.

Progress

Code Development

Twelve modifications to the SEAPODYM code have been completed since SC8. The two most significant modifications are capacity for sub-regional modelling at high resolution and the incorporation of tagging data.

Reference Fits

Reference fits using SODA 1 degree (1998-2008) and NCEP-ORCA2 2 degrees (1960-2008) physical forcing have been completed for skipjack, bigeye and south pacific albacore tuna. Reference fits using IPSL CMIP4 physical forcing have also been completed for skipjack, bigeye and south pacific albacore tuna for forecasting the impacts of climate change on tuna resources within the WCPO. In all reference fits the correspondence between the predicted and observed catch, length and CPUE was satisfactory for most of the fisheries defined. However for some fisheries the fit deteriorated over the last years of the optimisation. The estimation of diffusion rate was unsatisfactory for all models and was fixed at its upper boundary.

Current and Future Work Plan

Significant progress has been made on developing the first application of SEAPODYM to swordfish. Development of a second generation model will commence in December 2013 for this species which will incorporate updated fisheries data provided to the WCPFC for this species.

The incorporation of Pacific Ocean tagging data will commence once new physical forcing data (either SODA 1 degree and MERCATOR ¼ degree) are pre-processed for use in SEAPODYM. The revised SODA forcing should extend the modelling period to December 2009 and the MERCATOR forcing until December 2012. It is expected that new reference fits for each species will results through the applications of these new data sources (forcing and tagging).

The development of the model for yellowfin tuna will commence in the later 2013 with the incorporation of tagging and new physical forcing data.

The biomass estimates from exisitng reference fits for skipjack, bigeye and south pacific albacore tuna have been prepared for distribution to WCPFC members. Opportunistically, WCPFC members have been provided with initial training in interpreting and extracting these estimates.

The current physical forcing for the evaluation of climate change scenarios is restricted to a single CMIP4 model (IPSL). To capture the uncertainty in climate change projections an ensemble of CMIP5 models is being developed. For the historical period a revised physical forcing that has realistic simulation of oceanic conditions, under the influence of ENSO and PDO variability, has been generated. The coupled NEMO-PISCES model has been forced by observed winds of the ERA-Interim

reanalysis using the latest version (IFS5) covering the period 1979-present. Five to six CMIP5 models will be coupled with the NEMO-PISCES model to generate physical forcings under climate change. The choice of CMIP5 models has been determined by their compatibility with the historical forcing (so the jump from the historical forcing to the climate anomaly is minimised) and that they have realistic ENSO and PDO variability. This approach means that SEAPODYM only needs to be optimised once for each species before simulation of various climate change scenarios can be implemented.

The software SEAPODYMview which provides for easy display of SEAPODYM output is currently being revised to allow use on non-Linux operating systems and to provide improved visualisation options.

Acknowledgements and Donors

Project 62 is currently supported by 6 projects with financial support provided by Secretariat of the Pacific Community, Collecte Localisation Satellites, Australian Government Overseas Aid Program (AUSAID), 10th European Development Fund (EDF), Deutsche Gesellschaft für Internationale Zusammenarbeit (GIZ), Western Pacific Regional Fishery Management Council, Government of Indonesia, Agence Francais de Developpement, and Pelagic Fisheries Research Program. The Inter American Tropical Tuna Commission has provided access to non-public domain data for the purposes of progressing the work programme of the WCPFC-SC.

1. INTRODUCTION

SEAPODYM is a model developed for investigating spatial tuna population dynamics, under the influence of both fishing and environmental effects. The model is based on advection-diffusion-reaction equations, and population dynamics (spawning, movement, mortality) are constrained by environmental data (temperature, currents, primary production and dissolved oxygen concentration) and simulated distribution of mid-trophic (micronektonic tuna forage) functional groups. The model simulates tuna age-structured populations with length and weight relationships obtained from independent studies. Different life stages are considered: larvae, juveniles and (immature and mature) adults. After juvenile phase, fish become autonomous, i.e., they have their own movement (linked to their size and habitat) in addition to be transported by oceanic currents. Fish are considered immature until pre-defined age at first maturity and mature after this age, i.e., contributing to the spawning biomass and with their displacements controlled by a seasonal switch between feeding and spawning habitat, effective outside of the equatorial region where changes in the gradient of day length is marked enough and above a threshold value. The last age class is a "plus class" where all oldest individuals are accumulated. The model includes a representation of fisheries and predicts total catch and size frequency of catch by fleet when fishing data (catch and effort) are available. A Maximum Likelihood Estimation approach is used to optimize the model parameters. Additional information can be found in the references listed at the end of this document.

2. AFFILIATED PROJECTS

The continued development and application of the SEAPODYM model to the work of the WCPFC Scientific Committee is facilitated through Project 62. The project affiliates the independently funded work on SEAPODYM into the SC's work programme.

This modelling effort started in 1995 at the Secretariat of the Pacific Community in Noumea, New Caledonia, under two consecutive EU-funded projects: SPR-TRAMP (1995-2000) and PROCFISH (2002-2005). The model development also benefited of a grant (# 651438) from the PFRP (Pelagic Fisheries Research Program) of the University of Hawaii. Since 2006, the development has continued within the Space Oceanography Division of CLS, a subsidiary of the French CNES and IFREMER Institutes in collaboration with SPC (under the EU SCIFISH project and a grant from the Australian Department of Climate Change and Energy Efficiency) and PFRP (project number 657425, 659708 and 661551). Current projects are described in Table 2.1.

Table 2.1: Current projects and donors affiliated with Project 62.

Title	Purpose	Donor
Scientific Support for the Management of Coastal and Oceanic Fisheries in the Pacific Islands Region (SciCOFish)	Develop reference fits for the historical period for skipjack, bigeye and south pacific albacore. Develop reference fit for the IPSL CMIP4 model and provide first simulation of Climate Change Impacts for skipjack, bigeye and south pacific albacore	10th European Development Fund
SPC-Australian Climate Change Support Programme 2011-2013	Analysis of climate change impacts for skipjack, bigeye, yellowfin and south pacific albacore to assist national and regional policy formation	Australian Government Overseas Aid Program (AUSAID)
Enhanced estimates of climate change impacts on WCPO tuna, including estimates of uncertainty	Application of a model ensemble approach to capture the uncertainty in climate change forecasts for Pacific tuna populations	Deutsche Gesellschaft für Internationale Zusammenarbeit (GIZ)
Skipjack resource assessment for the Mariana Islands	High resolution modelling to estimate the skipjack resource status in the Mariana Islands	Western Pacific Regional Fishery Management Council
Integrating conventional and electronic tagging data into the spatial ecosystem and population model SEAPODYM	Modify the code of SEAPODYM to incorporate tagging data	Pelagic Fisheries Research Program
Infrastructure Development of Space Oceanography for IUU Fishing and Coral Monitoring (INDESO Project)	Modify the code to allow operational and sub-regional modelling	Government of Indonesia, Agence Française de Développement

3. CODE DEVELOPMENT

The code of SEAPODYM is continually enhanced to improve the model skills and to facilitate its use by non-developers colleagues. A major code development has been the inclusion of tagging data in the optimisation. Other changes since those reported at SC8 include:

a) Integration of dynamics equations over age was corrected to match exactly with the time step of simulations to increase the accuracy of model numerical solution.
b) The robustified log-likelihood has been implemented and is now used instead of normal log-likelihood for the length-frequencies data component in parameter estimation. Robustified log-likelihood accounts for the size and the variance of length-frequencies samples.
c) The code has been upgraded to allow running optimization tasks at higher temporal and spatial resolutions; the highest resolution being limited by those of the environmental forcing.
d) The fishing data resolution can be degraded to lower resolution if necessary. The interest of doing so is to account for a lack of good mesoscale representation or to reduce the biases due to the errors in the fine-resolution fishing data.

e) The adjoint code has been fully revised in order to enhance the computational efficiency of the code. Part of the adjoint routines were re-written to allow re-computation of variables instead of storing them in the gradient stack thus reducing the memory required to save variables to compute gradients by about 15%. This is a critical issue to enable higher spatial resolution runs and/or integration of more data (e.g., tagging) in the Maximum Likelihood Estimation (MLE). The code was also enhanced by avoiding Input/Output operations during optimization runs.

Various options and external routines were also developed to facilitate the use of the model and the analyses of simulations:

f) Options are now available to run various fishing effort scenarios based on spatial management measures. Using a mask file, EEZ or any area defined by a polygon can be closed to any fishery. The corresponding effort can be chosen to be lost; redistributed proportionally to CPUE outside the selected area, or transferred to another fishery (e.g. FAD to school sets). Example of application is provided in Sibert et al., (2012). Also, scenarios with increased fishing effort in the area of interest (defined by number codes in the mask file) can be simulated. Besides the possibility to select fisheries from the list, the user can also choose the mode of effort allocation within the given area: 1) proportional to existing effort; 2) homogeneous distribution.

g) Routines (R scripts) for the analysis of outputs at EEZ scale have been updated and now account for the exact area of the EEZ in each cell (i.e., surface area of partial cells are computed).

Several diagnostic routines were added to the code and routines were developed to facilitate the analysis and validation of simulation outputs:

h) Predicted mean mortality at age computed as weighted average by the density of cohort
i) Predicted mean diffusion rate at age and mean advection rate at age
j) Predicted density of larvae by SST bins, allowing an easy comparison with existing observations
k) Predicted timing in the seasonal switch between feeding and spawning migration according to latitude
l) Level of exploitation, based on the decrease of spawning (adult) biomass relatively to a virgin stock (i.e. a simulation without fishing mortality)
m) EEZ-level plots, showing seasonal variability of model variables within EEZ as well as observed vs. predicted data (mean catch and CPUE) within EEZ. The latter can be used as well for validation purposes.

4. INTEGRATION OF TAGGING DATA IN SEAPODYM OPTIMIZATION

A major area of development concerns the use of tagging data in the optimization approach of tuna population dynamics. The method to integrate conventional (release-recapture) tagging data has required substantial changes in the code structure. A test application of this code revision has been completed for Pacific skipjack with the constraint of physical forcing only being available until December 2008.

Technical code developments

Combining tagging data with SEAPODYM age-structured population model leads to augmentation of the model state vector through inclusion of variables describing the density of the cohorts of tags. Part of the adjoint code was rewritten in order to reduce the size of the memory required for saving the intermediate variables for computation of the cost function gradient. This allowed decrease of the gradient stack size by 15%. Also, the IO operations were eliminated completely from the runs with optimization. In addition, the code was adapted and recompiled with more recent versions of gcc4.4 and the AUTODIF library. This allowed allocation of more than 4Gb of RAM for computation of the cost function gradient.

Model description

Let us denote N(a,x,t) the population density at age a, where $x \in R^2$ and $t \in [t_0,t_n]$. Similarly, R(k,a,x,t) is the density of tags of k-th cohort; here the time $t \in [\tau_k,t_k]$ is defined by the time of release τ_k of k-th cohort and the time of recapture t_k within the modeled time interval. By definition the cohort of tags is the ensemble of individuals, tagged with conventional method, which were recaptured at the same time period (month – quarter, depending on the time scale chosen for the age structure). According to this definition, only the tags which were recaptured will be integrated into the model and hence drive the maximum likelihood estimation. This approach has been chosen to improve the estimation of habitat and movement parameters in SEAPODYM and these are the parameters, which are explicitly observed from conventional tagging data. It also avoid possible bias in the estimation of natural mortality due to misreporting problem or absence of fishing effort associated with tag recapture.

The model with tags is hence represented by the following system of PDE equations with initial and boundary conditions:

$$\partial_t N + \partial_a N = -div(\mathbf{v}N + \chi \nabla H \cdot N) + \nabla(D\nabla N) - (M+F)N;$$
$$\partial_t R + \partial_a R = -div(\mathbf{v}R + \chi \nabla H \cdot R) + \nabla(D\nabla R) + r(a,t,x);$$
$$N(a,x,t_0) = N_0(a,x); N(0,x,t) = H_s \cdot f(N_a), a > 0;$$
$$R(k,a,x,t_0) = 0$$
$$\mathbf{n} \cdot \mathbf{v}|_{x \in \partial\Omega} = \mathbf{n} \cdot \nabla N|_{x \in \partial\Omega} = \mathbf{n} \cdot \nabla R|_{x \in \partial\Omega} = 0$$

Hence, each population of tags has the same age structure as the actual population of modeled species; and the spatial and temporal dynamics are described with help of the same advection-diffusion equations with the reaction term set to zero (i.e., no recruit nor mortality) and the only reaction term is to account for the change of the density due to the tag releases within the cohort.

The equations for densities of tags R are solved numerically using the same ADI solver implemented in SEAPODYM.

Method Implementation

A new dimension was added to the existing population structure to allow simultaneous integration of PDE equations for as many tagged cohorts as specified in the parameter file. The life span of each cohort of tags is defined according to the age of youngest and oldest tagged individuals in a given cohort. The input files with tagging data must be prepared in the ASCII format, each file containing the data for one cohort: positions and time of release and recaptures and the length of fish at release. In case if tagging data are used in the optimization experiment, the likelihood function is augmented with the third component being the sum of errors of the predicted vs observed number of tags in the model grid cell.

Validation and sensitivity analysis

The validation of the approach included 1) the derivative check, which is necessary to assure that the derivative (adjoint) code is correct and 2) twin experiments which consist in creating pseudo-data sets for conventional data and running the model in optimization mode to test if the original solution used to create the artificial tagging data can be retrieved. Set of such experiments were done for the cases with minimization of the recapture likelihood only and compared with minimization of the full likelihood with catch, length and recapture components. The sensitivity analyses were done in order to reveal the parameters which can be estimated due to integration of the tagging data. As expected, the parameters driving the movement, i.e. maximal sustainable speed, diffusion, and movement habitat parameters have higher sensitivity (relative sensitivity > 5%, see Figure 4.1) when using tagging data in the likelihood. This result is also corroborated by the twin experiment study, showing that the optimal movement and habitat parameters can be retrieved even while minimizing the three-component likelihood function.

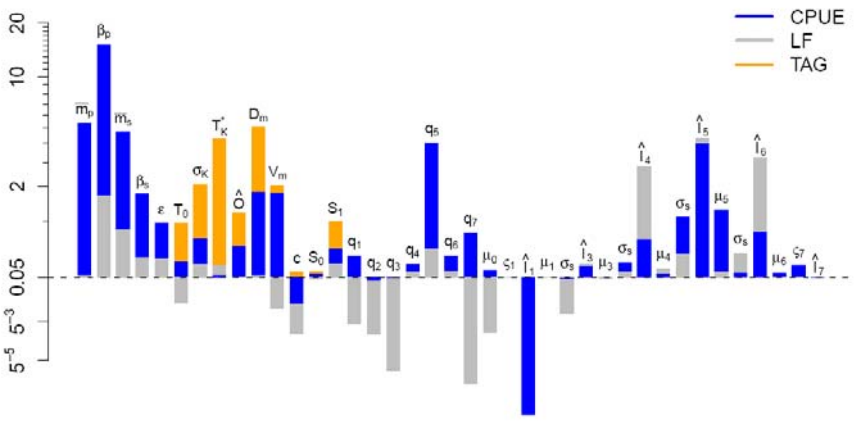

Figure 4.1: Results of sensitivity analysis for the experiment with 2008 tagging data. Each color corresponds to the sensitivity metrics obtained with single likelihood component.

Application to Pacific skipjack

Using compiled tagging datasets provided by NIFSF and SPC the cohorts of tags were defined. The first experiments were done for Pacific skipjack tuna on 1-degree and monthly resolution based on SODA physical forcing, VGPM primary production and Levitus climatological oxygen. Eight monthly tagged cohorts recaptured during 2008 were selected for these experiments (see the two examples with most contrasting movement patterns on Figure 4.2). The time period of model run was limited to 7/2006-12/2008 in order to cover entirely the observed time at liberty of tags released under PTTP tagging programme, which started in 2006.

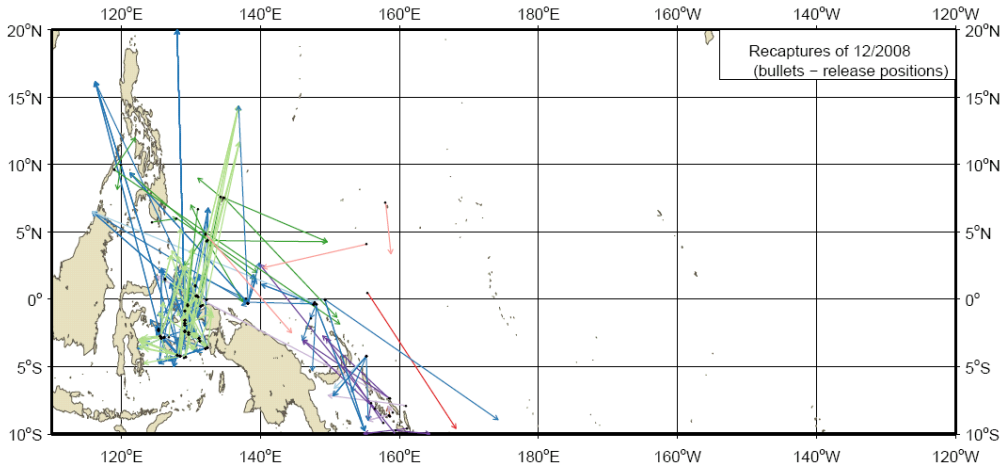

Figure 4.2: Cohorts of tags defined by the date of tag recaptures. Colours represent different cohorts of releases.

The optimization experiments with identical model configuration were performed with two- and three-component likelihood. The results show that integration of tagging data leads to estimation of smaller diffusion and much higher advection rates (see Table 4.1), which results in less spread-out distribution of skipjack (Figure 4.3) and hence much smaller total biomass (4 vs. 10 million tonnes in this experiment). However, it is too early to assert that this estimate is better than the one obtained with catch data only, since the 2.5 years time period used for this experiment is not long enough to get reliable estimates of total stock.

Table 4.1: Control parameter estimates for skipjack using 2006-2008 time period and likelihood components with catch and catch and tags data

Parameters estimated by the model			Unit	Value	
				L_catch	L_catch + L_tags
T_s	Spawning	Optimum of the spawning temperature function	°C	31.3	31.35
σ_s		Std. Err. of the spawning temperature function	°C	2.25*	2.25*
T_a	Feeding habitat	Optimum of the adult temperature function at maximum age	°C	18]	18]
σ_a		Std. Err. of the adult temperature function at maximum age	°C	4.5]	4.5]
$\hat{O}$		Oxygen threshold value at Ψ_O =0.5	mL · L^{-1}	2.19	3.13
M_p		Slope coefficient in predation mortality		0.09	0.03
M_{max}		Maximal mortality rate due to predation	month^{-1}	0.5]	0.35
M_s		Slope coefficient in senescence mortality		1.98	1.94
D_{max}	Movement	Diffusion parameter		0.15]	0.11
V_{max}		Maximum sustainable speed	B.L. s^{-1}	0.53	4.43

[val = value close to minimum boundary value; val] = value close to maximum boundary value,
*=fixed

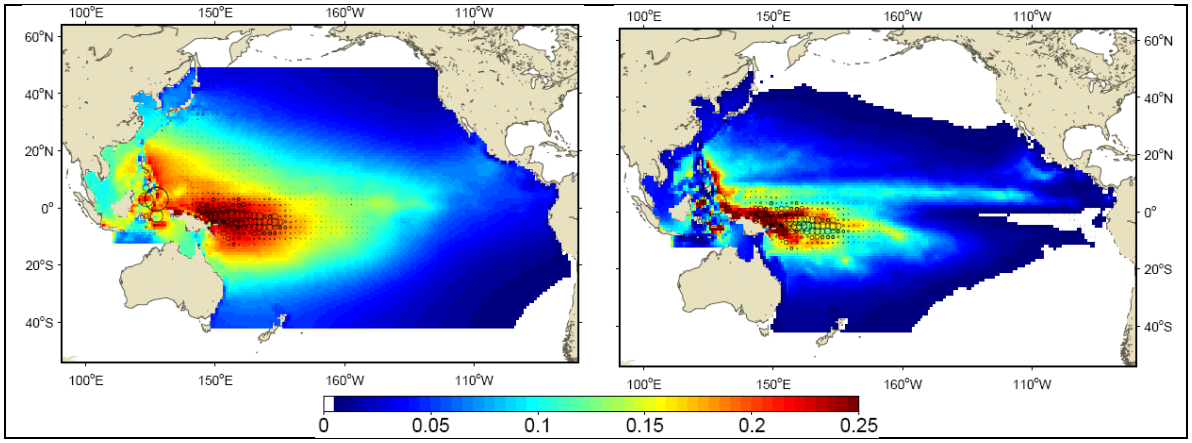

Figure 4.3: Predicted distributions of skipjack tuna (average of 2007 and 2008) in g/m2 (both young and adult life stages) as the result of experiments conducted with different likelihood composition: (left) including CPUE and length frequencies components only; (right) CPUE, LF and tagging data.

5. REFERENCE FIT FOR PACIFIC SKIPJACK FOR THE HISTORICAL PERIOD (SKJ2.1 SODA-v2.1)

Physical forcing: SODA reanalysis

Reference fits for skipjack were achieved using a new release of the SODA (Carton et al. 2000; http://soda.tamu.edu/) ocean physical reanalysis and satellite derived primary production. Due to data assimilation techniques and the use of satellites data, this environmental forcing is more realistic than previous forcings used from coupled physical biogeochemical models. However, the series is limited to the period 1998-2008. The resolution is 1° x 1° x month. The necessary variables (temperature, currents, primary production and euphotic depth) were processed using the model definition of vertical layers (linked to the euphotic depth) and used to produce the biomass distributions of the 6 micronekton functional groups. Monthly climatological data from the World Ocean Atlas (WOA2010) were used for the dissolved oxygen concentration.

Initial conditions were required for this analyses (biomass and distribution) and this was achieved using a ORCA2 hindcast simulation (1958-2008). Both past climatic and fishing mortality define the initial conditions of the stock when starting a simulation at any given date. Unfortunately, the lack of historical synoptic datasets for oceanic physical variables before the 1980s, and before 1998 for the ocean color (i.e., SeaWiFS), ocean reanalyses are not available to simulate tuna dynamics with SEAPODYM for periods before 1998. As an alternative, hindcast simulations with coupled ocean physical-biogeochemical models can be used. These simulations are forced by atmospheric data for which a few reanalyses are available (e.g. NCEP, ERA40). To produce the initial conditions used for the reference configuration the biogeochemical model is PISCES (Pelagic Interaction Scheme for Carbon and Ecosystem Studies; Aumont and Bopp, 2006) was used. It incorporates both multi-nutrient limitation (NO3, NH_4, PO_4, SiO_3 and Fe) and a description of the plankton community structure with four plankton functional groups (Diatoms, Nano-phytoplankton, Micro-zooplankton and Meso-zooplankton). PISCES is coupled to the ORCA2 configuration of the ocean circulation model OPA (http://www.nemo-ocean.eu/), and driven by the NCEP-NCAR reanalysis, that provides 50-year record of global analyses of atmospheric fields based on the recovery of land surface, ship, rawinsonde, pibal, aircraft, satellite, and other data. (http://www.cgd.ucar.edu/cas/guide/Data/ncep-ncar_reanalysis.html). This hindcast simulates reasonable seasonal, interannual and decadal variability at basin-scale at a coarse resolution of 2°x2°x month.

Fishing data

A new dataset of fishing data was used for skipjack fisheries in the WCPFC (Table 5.1). Except for the Philippine-Indonesia fishery and the longline fishery, all catch and effort fishing data were at a resolution of 1°x1°x month, which is a major improvement from the previous studies where these data were at a 5°x5° resolution. Based on discussion with Japanese colleagues, the two Japanese pole and line (P1 and P2) were revised to describe small and large pole-and-line boats rather than western and central fleets. Philippines and Indonesia fleets have been combined and not used in the optimization approach due to a lack of accuracy.

Table 5.1. Updated fisheries definition for skipjack

Id	Gear	Region	Description	Nationality	C/E data month/year	Reso-lution	Size data qtr/year	Reso-lution
P1	PL	15N-45N; 115E-150W	PL Small pole & Line	Japan	1/1972 - 12/2008	1x1	1/1964 – 12/2008	5x5
P2	PL	25N-45N; 165E-150W	PL Large pole & line	Japan	6/1972 - 12/2008	1x1	2/1972 – 12/2008	5x5
P3	PL	15S-0; 140E-165E	Pole and line	Papua New Guinea & Solomon Islands	3/1970 - 12/2008	1x1	3/1984 – 12/2008	5x5, 10x20
S4	PS	25N-45N; 140E-165E	PS subtropical fishery	Japan	7/1970 - 12/2008	1x1	2/1974 - 4/2008	5x5
S5	PS	20S-15N; 130E-150W	PS on LOG	All	11/1970 - 12/2008	1x1	2/1988 - 12/2008	5x5, 10x20
S6	PS	20S-15N; 130E-150W	PS on FAD	All	11/1970 - 12/2008	1x1	3/1988 - 12/2008	5x5, 10x20
S7	PS	20S-15N; 130E-150W	PS on free school	All	12/1967 - 12/2008	1x1	4/1987 - 12/2008	5x5, 10x20
L8	LL	20S-25N; 115E-150W	LL exploratory fishery	Japan	6/1950 - 12/2008	5x5	1/1970 - 3/2008	5x5
D9	DOM	10S-15N; 115E-130E	mixed set types	Philippines & Indonesia	1/1970 - 12/2008	5x5	1/1970 - 12/2008	region
S10	PS	EPO	PS on Dolphin schools	NA	10/1959-8/2007	1x1	1/1961 – 4/2005	EPO
S11	PS	EPO	PS on Floating objects	NA	7/1959 – 8/2007	1x1	1/1961 - 4/2005	EPO
S12	PS	EPO	PS on free school	NA	3/1959-8/2007	1x1	1/1961 - 4/2005	EPO
P13	PL	20S-5N; 175E-185E	Pole and Line	Fiji	1/1976 - 12/2007	5x5	4/1991 - 12/2007	5x5, 10x20

Optimization experiments

The likelihood optimization was performed on the dataset from 2000-2007 time period. The model results were validated using the whole time series, i.e. 1999-2008. Model parameters could not be optimized all together due to the lack of signal in the fishing data to constrain the antagonistic and correlated mechanisms, e.g., mortality and recruitment. A series of optimization experiments was carried out to test different model configurations and time periods with fixed length-at-age, recruitment and mortality coefficients of early life stages. Despite a relatively short time series (10 years), the estimation of the habitat parameters and the spatial solution was very stable among all experiments being strongly constrained by environment provided by SODA reanalysis, satellite derived primary production and by the spatial signal from CPUE and LF data.

Since the objective is to produce a reference fit that can be used to answer various spatial management issues, it was decided to constrain the recruitment by the MULTIFAN-CL (MFCL) estimate and to impose the limits on the mortality parameters to keep them in proximity to MFCL estimates.

Skipjack population structure

The structure of the population was defined by age (cohorts) with variable time unit allowing to save computation time. There is 1-month cohort for larvae life stage, one 2-month cohort for juvenile

stage, five 1-month and one 2-month cohorts for young fish (before age at maturity) and 9 cohorts for adult stages (two of 2 months, two of 3 months and the last five of 4, 5, 6, 7, 9 months correspondingly). The last "+ cohort" accumulates older fish. Age at maturity is set to 10 months. Age-length and age-weight relationships (Fig. 6.1) are derived from the last MULTIFAN-CL estimate (Hoyle et al., 2011).

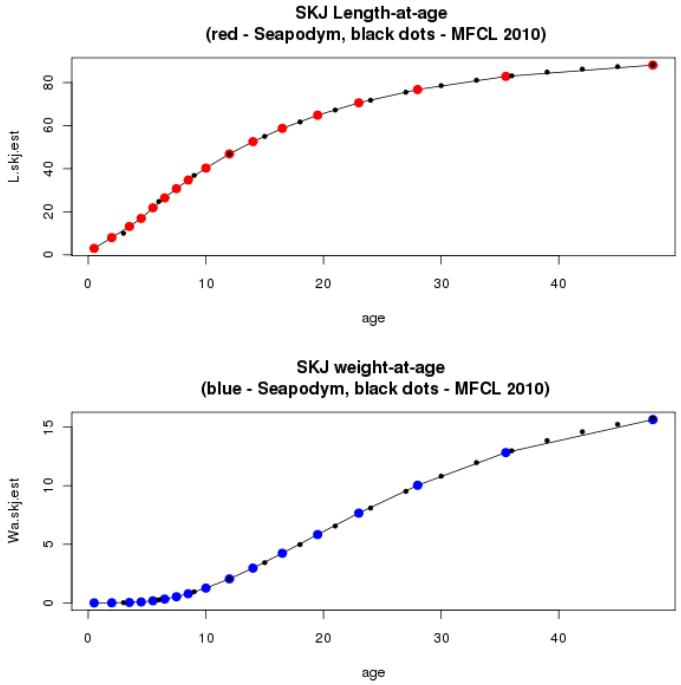

Figure 5.1. Skipjack size (FL in cm) at age (month) and weight (kg) at age functions used in SEAPODYM simulation, based on MULTIFAN-CL 2010 and 2011 estimates (Hoyle et al, 2011)

Fit to catch data

The spatial CPUE and length-frequencies data contributed to the total likelihood function. Overall spatial fit to predicted catch is close to the previous solution with SODA reanalysis 2.4 but a significant improvement is particularly visible for the eastern Pacific fisheries (Figure 5.2).

Catchability by fishery was estimated to increase since 1998 for the western purse seine fisheries (

Table 5.2) with the largest annual increase for the FAD and LOG fisheries (+3.6%) followed by the free school fishery (+1.6%). Conversely, in the eastern Pacific the catchability of the purse seine fishery on floating objects is estimated to have decreased since 1998 with an annual decrease of 1.8%.

Selectivity coefficients (Fig. 5.3) were obtained with all parameters being estimated within their bounds. These selectivity estimates allowed a good fit with size frequency data for all fisheries. The fit to length frequency data is reasonable for all fisheries (Fig 5.4) with fisheries P1 (Japanese small pole-and-line boats) and S11 (eastern Pacific FAD-associated sets) showing a mode peaking in the smallest sizes while occasional catch in the longline fishery consisted of very large individuals.

The total catch of all fisheries is well predicted until 2003 but the correlation in fluctuations decreases after this year, though in average the predicted total catch remains consistent with observed catch. It appears that this lower correlation is due mainly to the fit for purse seine fisheries of the western Pacific using either Log of FAD (S5 and S6), especially during 2003-04, while predicted CPUEs of other fisheries correlated fairly well with observations (Figure 5.4). Reasons for this lack of fit are still unclear and need further investigation, but one explanation could be that the estimate was forced to be scaled to the MULTIFAN-CL biomass of region 2 (see below), thus leading to too high depletion in this area given the very strong fishing effort deployed there.

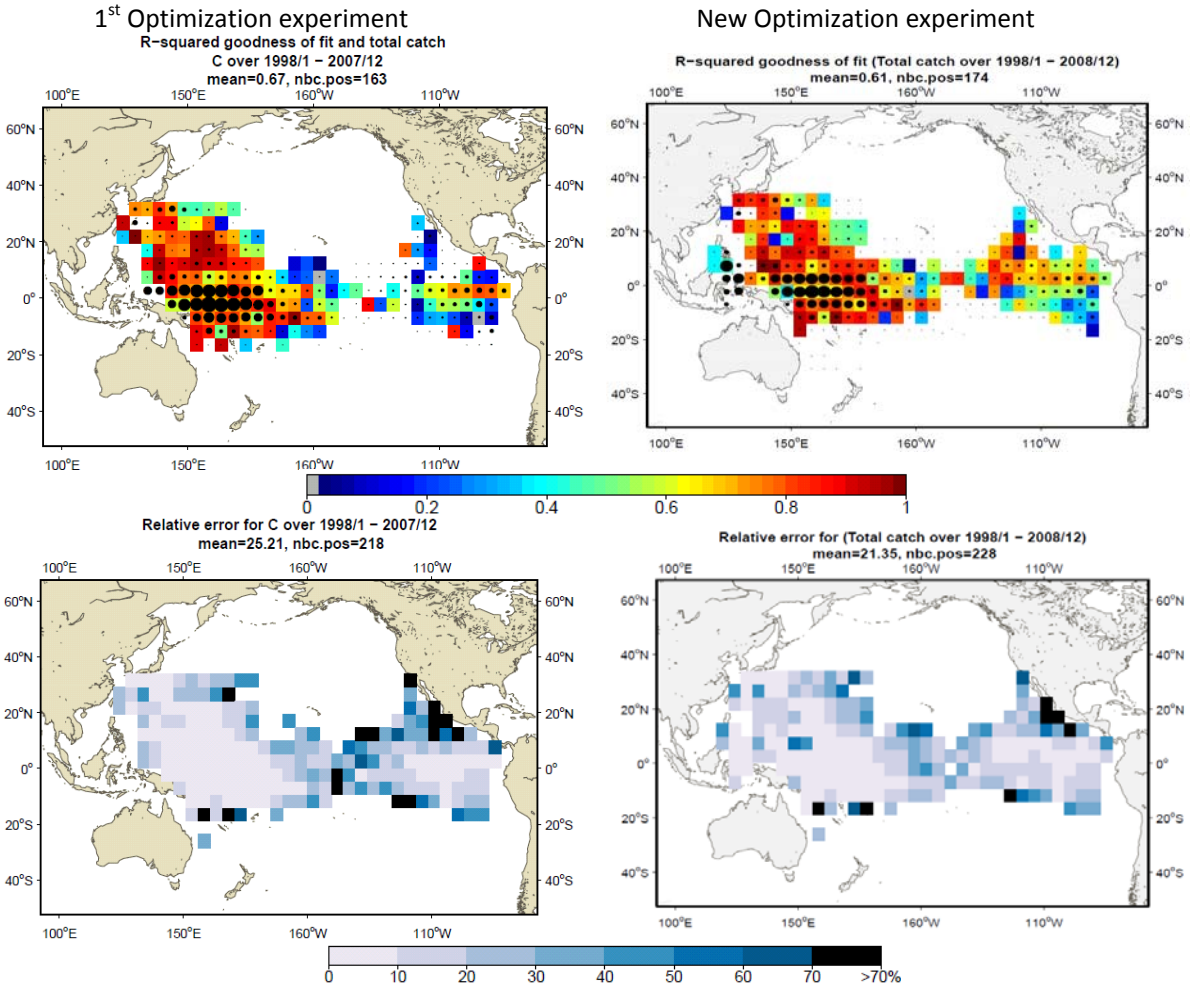

Figure 5.2. Comparison of fit to fishing data between previous (Lehodey et al. 2011) and new optimization experiments over all the period 1998-2008 with SODA-Psat environmental forcing. From top to bottom: R-squared goodness of fit and relative error in predicted catch for all fisheries; Black circles are proportional to the level of catch.

Table 5.2. Estimates of catchability by fishery and annual increase (%) since 1998.

Fishery		Q	slope	annual % change since 1998
P1	PL small boats	0.01128	0.00000	0.0%
P2	PL large boats	0.00797	0.00000	0.0%
P3	Pole and line PNG+ SOL	0.00901	0.00000	0.0%
S4	PS subtropical	0.16297	0.00000	0.0%
S5	PS on LOG	0.04395	0.00300	3.6%
S6	PS on FAD	0.04245	0.00300	3.6%
S7	PS on free school	0.04191	0.00100	1.2%
L8	LL exploratory fishery	0.00012	-0.00050	-0.6%
D9	mixed set types	0.00400	0.00100	1.2%
S10	PS on Dolphin schools	0.00335	0.00075	0.9%
S11	PS on Floating objects	0.04681	-0.00150	-1.8%
S12	PS on free school	0.04642	0.00000	0.0%
P13	Pole and Line	0.00710	0.00000	0.0%

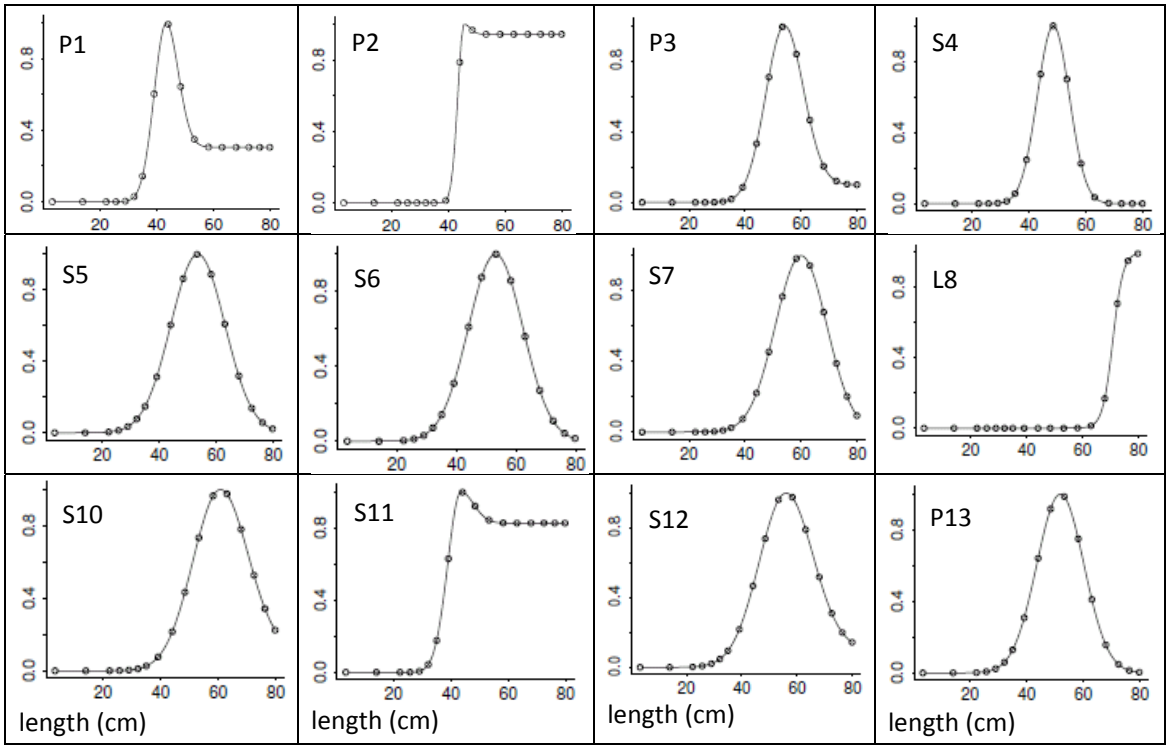

Figure 5.3. Optimized functions of selectivity by fishery.

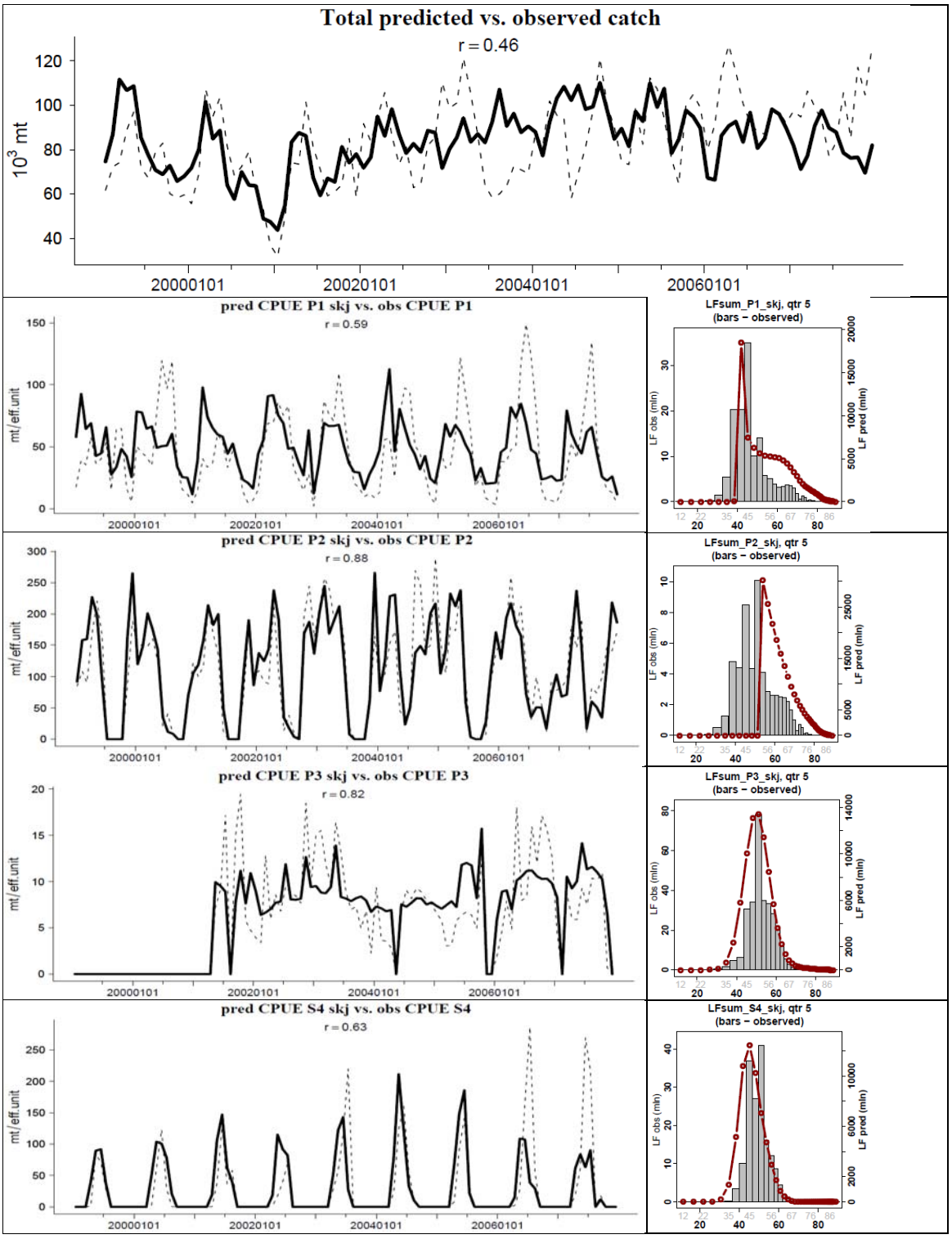
Total predicted vs. observed catch
r = 0.46
10^3 mt
120
100
80
60
40
20000101
20020101
20040101
20060101
pred CPUE P1 skj vs. obs CPUE P1
r = 0.59
mt/eff.unit
LFsum_P1_skj, qtr 5
(bars – observed)
LF obs (mln)
LF pred (mln)
pred CPUE P2 skj vs. obs CPUE P2
r = 0.88
LFsum_P2_skj, qtr 5
(bars – observed)
pred CPUE P3 skj vs. obs CPUE P3
r = 0.82
LFsum_P3_skj, qtr 5
(bars – observed)
pred CPUE S4 skj vs. obs CPUE S4
r = 0.63
LFsum_S4_skj, qtr 5
(bars – observed)

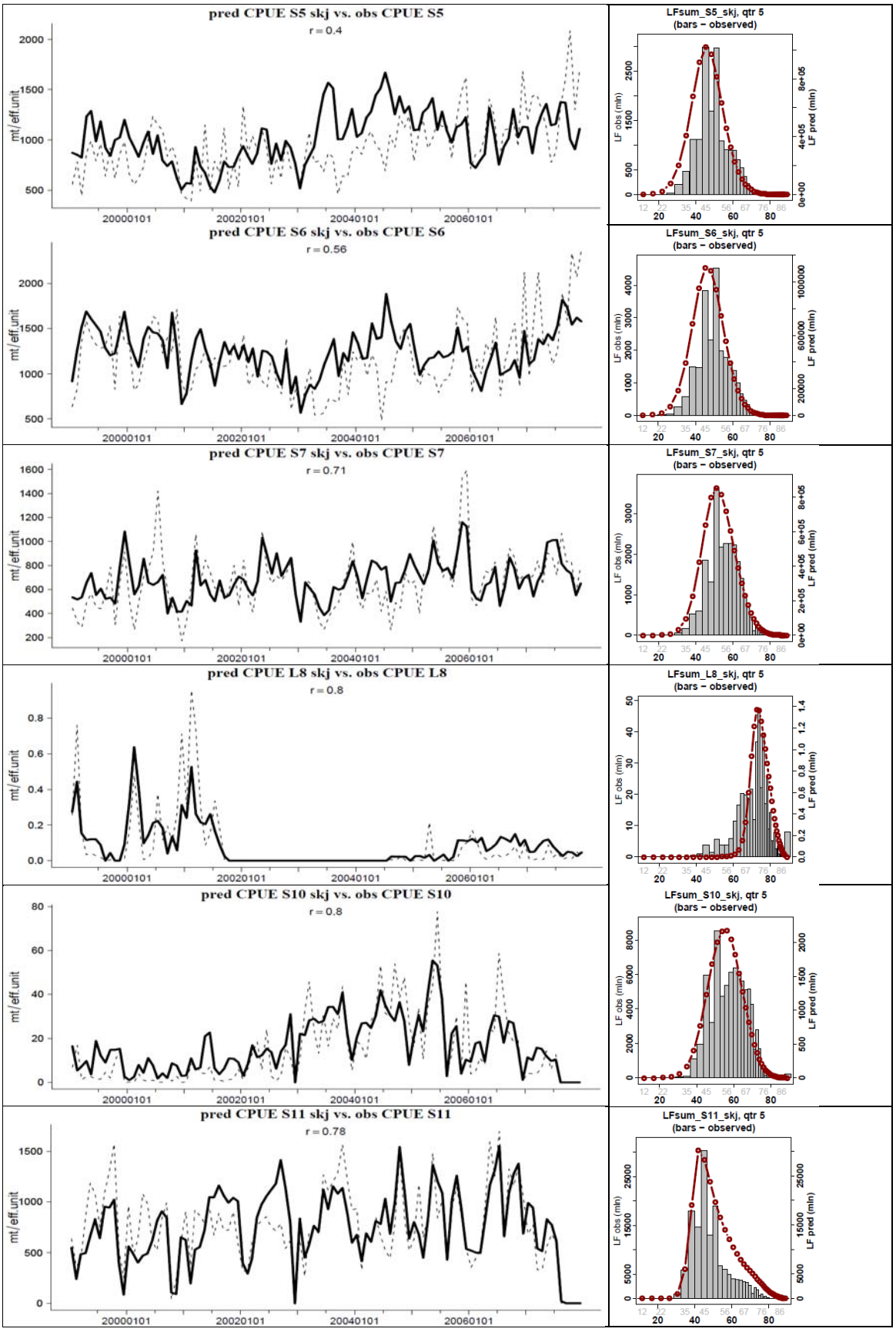
pred CPUE S5 skj vs. obs CPUE S5
r = 0.4
mt/eff.unit
20000101
20020101
20040101
20060101
LFsum_S5_skj, qtr 5
(bars – observed)
LF obs (min)
LF pred (min)
pred CPUE S6 skj vs. obs CPUE S6
r = 0.56
LFsum_S6_skj, qtr 5
(bars – observed)
pred CPUE S7 skj vs. obs CPUE S7
r = 0.71
LFsum_S7_skj, qtr 5
(bars – observed)
pred CPUE L8 skj vs. obs CPUE L8
r = 0.8
LFsum_L8_skj, qtr 5
(bars – observed)
pred CPUE S10 skj vs. obs CPUE S10
r = 0.8
LFsum_S10_skj, qtr 5
(bars – observed)
pred CPUE S11 skj vs. obs CPUE S11
r = 0.78
LFsum_S11_skj, qtr 5
(bars – observed)

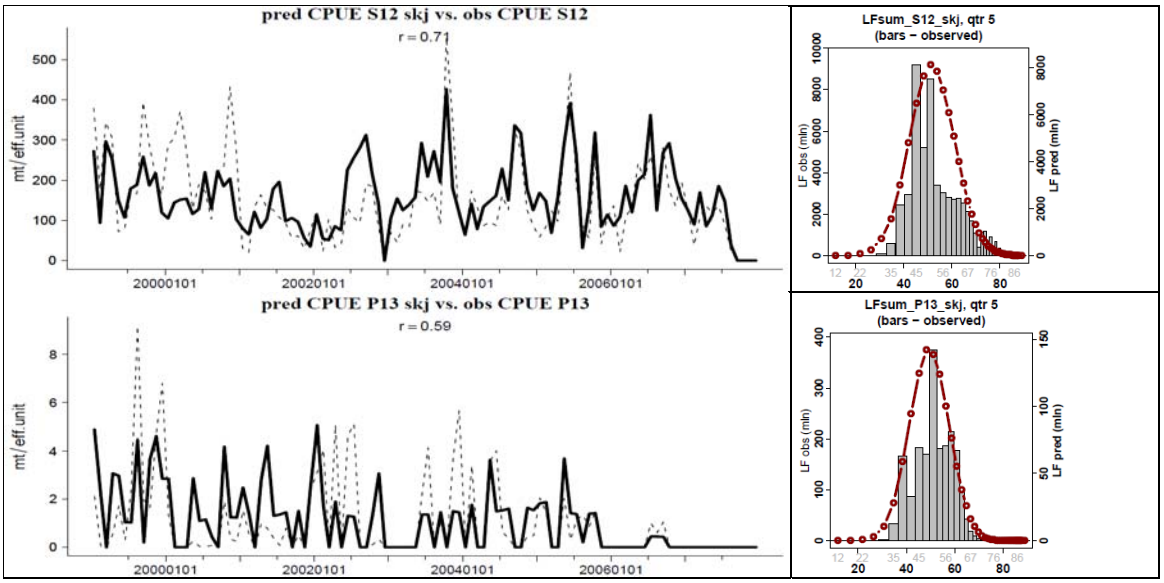

Figure 5.4. Total predicted (continuous line) and observed (dotted line) skipjack catch rates (CPUEs) and size frequencies.

Optimal Parameterization

The optimization was not able to correctly estimate some of parameters for habitat and movements (Table 5.3). Optimum of the spawning temperature function and its standard error, and the diffusion parameter were fixed. A wider range of temperature was fixed for the spawning function. The standard error of the adult temperature function at maximum age and the maximum sustainable speed were estimated near their upper and lower boundaries respectively.

Table 5.3: Habitats and movement parameter estimates for skipjack application

Parameters estimated by the model			**Unit**	**SODA 1° v1**	**SODA 1° v2**
T_s	Spawning	Optimum of the spawning temperature function	°C	28.67	29.5*
σ_s		Std. Err. of the spawning temperature function	°C	0.75*	3.0*
α		Larvae food-predator trade-off coefficient	-	1.03	0.51
T_a	Feeding habitat	Optimum of the adult temperature function at maximum age	°C	20.64	20
σ_a		Std. Err. of the adult temperature function at maximum age	°C	4.5]	3.5]
$\hat{O}$		Oxygen threshold value at Ψ_O =0.5	mL · L^{-1}	2.47	2.2
D_{max}	Move-ment	Diffusion parameter		0.065*	0.08*
V_{max}		Maximum sustainable speed	B.L. s^{-1}	[0.9	[0.75

*Fixed; [val = value close to minimum boundary value; val] = value close to maximum boundary value

Natural mortality

Natural mortality in SEAPODYM is estimated with an average mortality coefficient by cohort, and variability is allowed around this average value according to an index for food requirement and competition (Figure 5.5). This is a major difference in the representation of this key population

dynamics parameter in comparison to MUTLIFAN-CL. Due to such variability and depending on its estimated range the local mortality rates estimated in SEAPODYM can be very different from the average value. To estimate the actual average mortality rates resulting from these mechanisms for each cohort, the weighted means of variable mortality coefficients, with the weights being the cohort density, were computed. These weighted means are much closer to what is estimated by MULTIFAN-CL, with lower values due to the representation of fish movements in the model allowing fish to escape unfavourable habitats (with higher mortality rates) and concentrate in good habitats (with lower mortality rates). The main discrepancy between both models is an opposite trend in the early life stages with MFCL values increasing from juvenile to young cohorts before decreasing and converging with SEAPODYM estimates. This sort of trend is not permitted in SEAPODYM that assumes much higher mortality of larvae and juveniles stages than in older stages.

Spawning and larval recruitment

Optimal spawning temperature (SST) was fixed at 29.5 °C with standard error being 3.0 °C. This resulted in a predicted distribution of larvae starting to be abundant in water with SST above 25-26°C as proposed in the literature (Figure 5.6). The model estimate for the seasonal timing of spawning migration indicates that the switch from feeding to spawning habitat controlling the movement of fish peaks at Julian date ~5 (5 January) in the north hemisphere, but in latitude higher than 35° (Figure 5.6). Since this latitude corresponds to the extreme range of the species habitat (Figure 5.2), this mechanism has very limited impact. Movements of fish between latitude 35° north and south, i.e., most of the stock, is always controlled by the feeding habitat while spawning occurs year-round opportunistically and proportionally to the spawning habitat index and the density of adult fish (Figure 5.6), following the larval stock-recruitment relationship expressed in SEAPODYM, ie at the cell level.

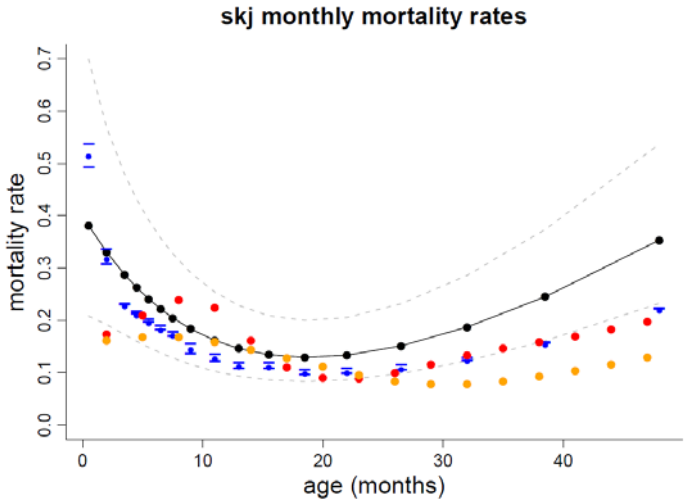

Figure 5.5: Natural mortality rates (month^{-1}) estimated from SEAPODYM optimization experiments. Black dotted line corresponds to the theoretical average mortality curve whereas blue dots indicate the mean mortality rates weighted by the cohort density and orange and red dots are the MUTLTIFAN-CL estimates for 2010 and 2011 assessments.

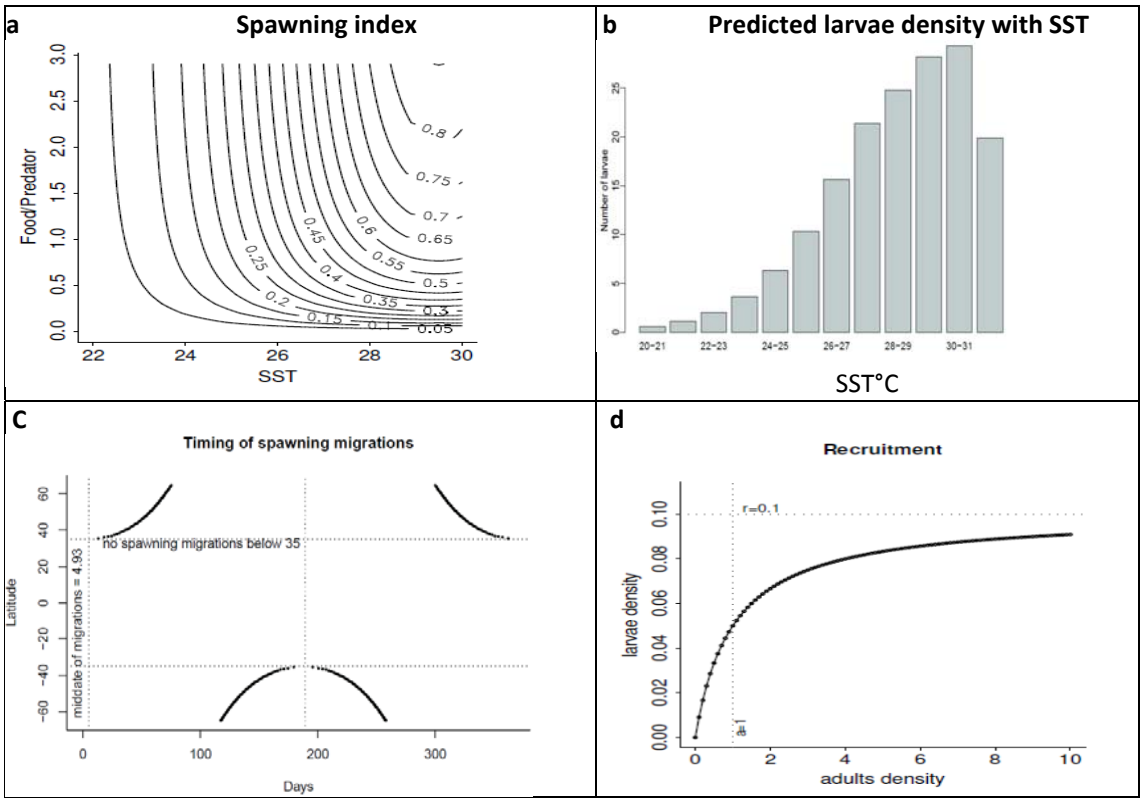

Figure 5.6: Spawning and larval recruitment. **a:** spawning index in relation to SST and food-predator tradeoff ratio. **b:** Distribution of larvae according to SST and the estimated parameters of spawning index. **c**: Seasonal timing of spawning migration. **d:** SEAPODYM larval stock-recruitment relationship estimated for skipjack. Densities are in number of individual per km^2 for adult and 1000's of individual per km^2 for larvae.

Feeding Habitat

The optimal value for the oldest cohort was estimated at 20 °C but the standard error reached the maximum fixed boundary (3.5 °C). The threshold value for the oxygen tolerance reached the minimum fixed 2.2 ml/l (Figure 5.7).

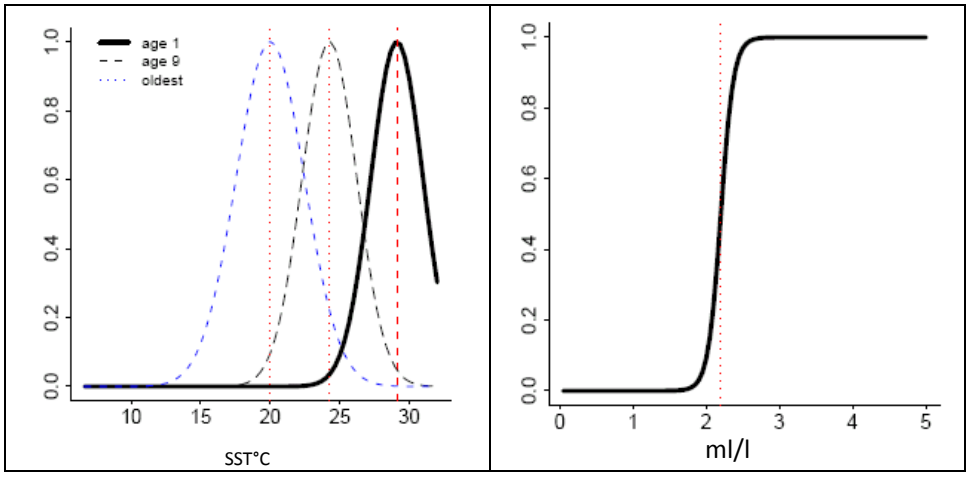

Figure 5.7: Optimized functions for temperature and oxygen habitats.

Movements

The value for maximum sustainable speed was estimated to 0.75 body length/s and the estimate for the diffusion coefficient for fish movements reached the upper boundary. Thus movement parameter optimization is not yet fully satisfactory. Estimation of diffusion coefficient is a key issue as high diffusion can quickly lead to overestimation of biomass. Further ongoing progress to use higher resolution and tagging data in the likelihood approach should be a major step for resolving this recurrent issue. When weighted by the cohort density, maximum diffusion rates remain below 700 nmi^2 $month^{-1}$ and the mean of maximum sustainable speed (in BL/s) shows an exponential decrease with age (size) which is linked to the increasing accessibility with age (size) to forage biomass of deeper layers, thereby decreasing the horizontal gradients of the feeding habitat index controlling the movement (Figure 5.8).

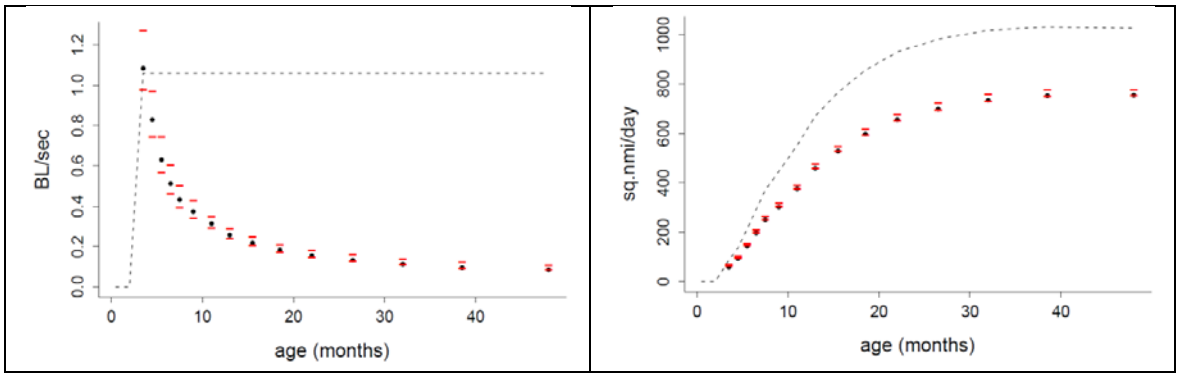

Figure 5.8: Maximum speed and diffusion rates by cohort (depending of age/size and habitat value / gradient) based on SEAPODYM parameterization (dotted lines) and predicted means weighted by the cohort density (black dots) with one standard error (red bars).

Biomass estimates and population dynamics

In average, spawning grounds and larvae are predicted to concentrate in the warm waters of the equatorial (10°N-10°S) western central Pacific Ocean with a prolongation of a relatively favourable habitat between 5°N and 10°N reaching the eastern Pacific coast (Figure 5.9). Distribution of young immature fish (until 42 cm) is very close to this distribution while adult fish extend their habitat towards central and eastern Pacific where they are caught occasionally by longline fisheries, and towards medium latitudes, especially under the influence of circulation of the warm western boundary currents: the Kuroshio and the Eastern Australian Currents.

There are a few regions where high biomass is due to obvious spurious accumulation, especially in the Arafura Sea. The biomass in the South China Sea seems also overestimated given the level of catch in this region. This is due to regions with shallow bathymetry and complex topography for which 1° resolution is insufficient to be realistic. This is particularly the case for the western boundaries of the model domain within the South-East Asia region.

The diffusion used to simulate random dispersion of fish may be also a source of overestimation of biomass in areas where there is no fishing data to bring information in the Maximum Likelihood Estimation. The result can be a smoothing of the contrast between higher and lower productive regions.

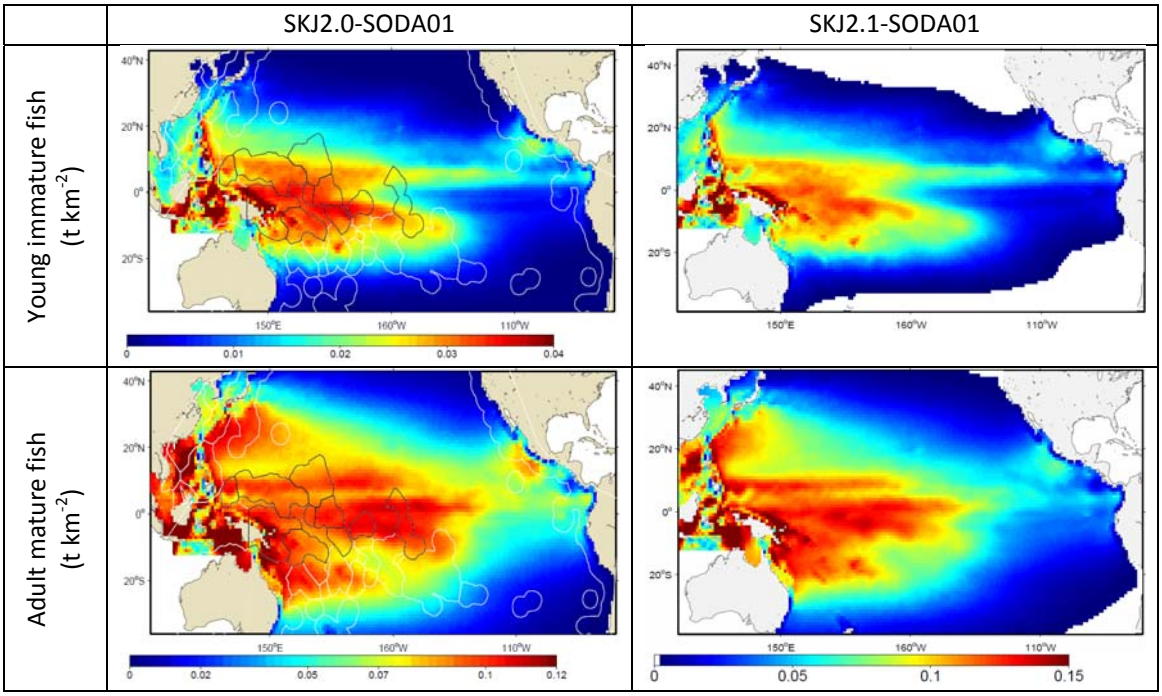

Figure 5.9. Change in average biomass distribution between first and revised reference fits using SODA configuration (here without fishing).

The revised reference fit for skipjack is characterized by reduction of total biomass with respect to previous estimate, which is more noticeable in EPO (see Fig. 5.5). However, this solution demonstrates similar variability of the stock. The skipjack spawning biomass in WCPO is estimated around 4 million metric tons, lower than MFCL prediction in this area (Fig. 5.10). The variability predicted over the last decade is still stronger in MFCL and driven by recruitment estimates. Though the average level of both biomass estimates is similar at the scale of the WPCO, there are regional differences. In both models the lowest biomass occurs in region 1 (north west Pacific) with MFCL estimate roughly 30-50% below the SEAPODYM estimate. However to be comparable, a data mask restricted to just the spatial areas where fishing occurs in region 1 should be applied when extracting the biomass estimates from SEAPODYM. As the fishing data is very restricted spatially in this region it is not unexpected that the MFCL estimate of biomass is smaller (ie. there is little data for MFCL to estimate biomass). The highest biomass is estimated in region 3 (central equatorial region) for MFCL but region 2 for SEAPODYM. The amplitude of fluctuation in biomass are always much larger in MFCL (Fig. 5.10).

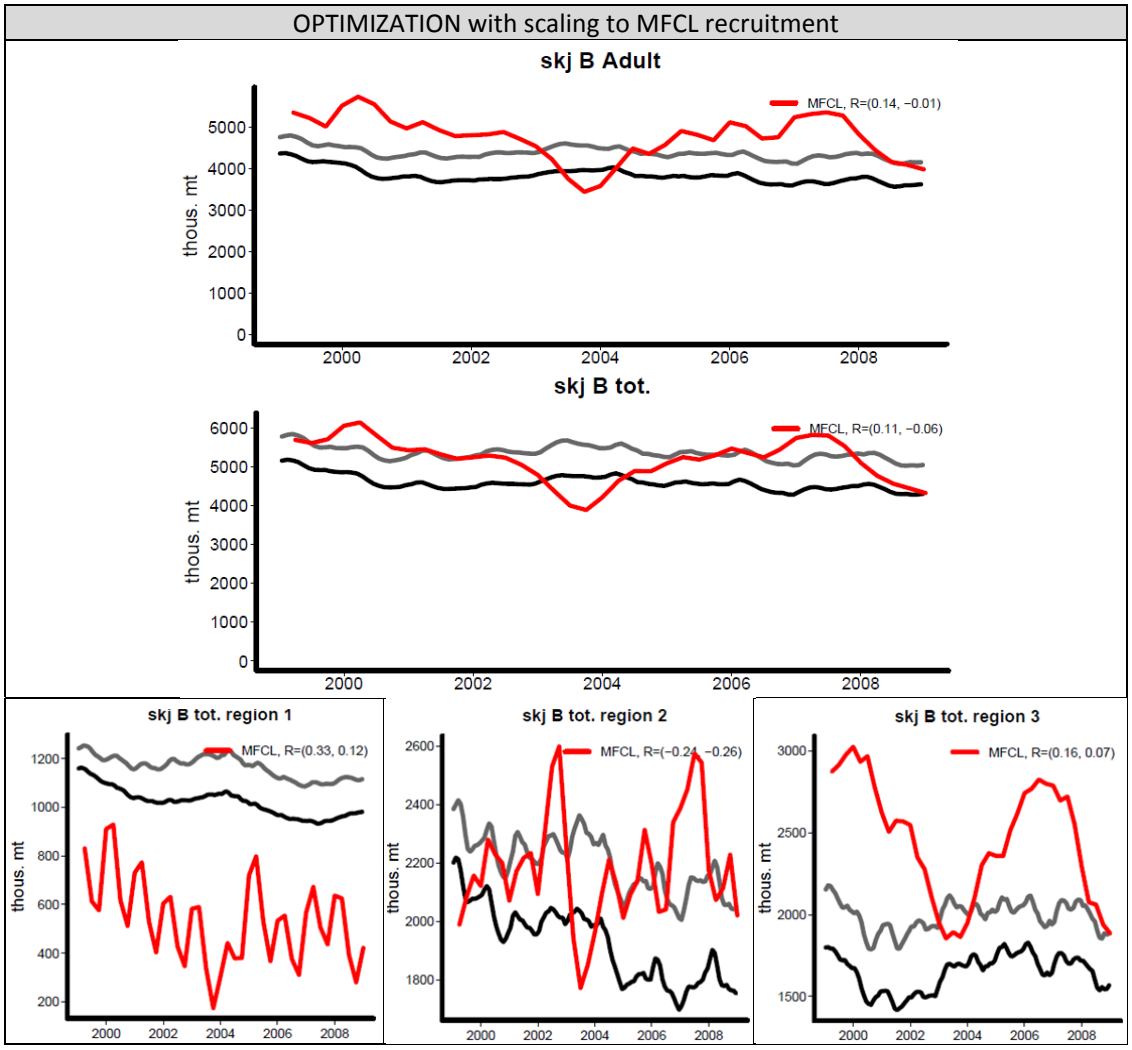

Figure 5.10. Comparison between SEAPODYM (1st and 2nd optimization in grey and black respectively) and MULTIFAN-CL (red curves) recruitment, spawning biomass and total skipjack biomass estimates for WCPO and by region 1 to 3.

6. REFERENCE FIT FOR PACIFIC BIGEYE FOR THE HISTORICAL PERIOD (BET2.0 SODA-v2.1)

Physical forcing: SODA reanalysis

Reference fits for bigeye were achieved using a new release of the SODA (Carton et al. 2000; http://soda.tamu.edu/) ocean physical reanalysis and satellite derived primary production. Due to data assimilation techniques and the use of satellites data, this environmental forcing is much more realistic than previous forcings used from coupled physical biogeochemical models. The series is limited to the period 1998-2008. The resolution is 1° x 1° x month. The necessary variables (temperature, currents, primary production and euphotic depth) were processed using the model definition of vertical layers (linked to the euphotic depth) and used to produce the biomass distributions of the 6 micronekton functional groups. Monthly climatological data from the World Ocean Atlas (WOA2010) were used for the dissolved oxygen concentration.

Initial conditions were required for this analysis (biomass and distribution) and this was achieved using a ORCA2 hindcast simulation (1958-2008). Both past climatic and fishing mortality define the initial conditions of the stock when starting a simulation at any given date. Unfortunately, the lack of historical synoptic datasets for oceanic physical variables before the 1980s, and before 1998 for the ocean color (i.e., SeaWiFS), ocean reanalyses are not available to simulate tuna dynamics with SEAPODYM for periods before 1998. As an alternative, hindcast simulations with coupled ocean physical-biogeochemical models can be used. These simulations are forced by atmospheric data for which a few reanalyses are available (e.g. NCEP, ERA40). To produce the initial conditions used for the reference configuration the biogeochemical model is PISCES (Pelagic Interaction Scheme for Carbon and Ecosystem Studies; Aumont and Bopp, 2006) was used. It incorporates both multi-nutrient limitation (NO3, NH_4, PO_4, SiO_3 and Fe) and a description of the plankton community structure with four plankton functional groups (Diatoms, Nano-phytoplankton, Micro-zooplankton and Meso-zooplankton). PISCES is coupled to the ORCA2 configuration of the ocean circulation model OPA (http://www.nemo-ocean.eu/), and driven by the NCEP-NCAR reanalysis, that provides 50-year record of global analyses of atmospheric fields based on the recovery of land surface, ship, rawinsonde, pibal, aircraft, satellite, and other data. (http://www.cgd.ucar.edu/cas/guide/Data/ncep-ncar_reanalysis.html). This hindcast simulates reasonable seasonal, interannual and decadal variability at basin-scale at a coarse resolution of 2°x2°x month. The time period 1980-2008 was used for optimization.

Fishing data

The definition of fisheries for bigeye tuna is provided in Table 6.1. The traditional longline fishery was divided into western (L1) and central (L22) Pacific longline fishery (Table 5.1). Also given the small amount of bigeye catch in the dolphin associated purse seine fishery in the EPO, this fleet was merged with the non-associated purse seine fleet (S17). All longline catch and effort fishing data are at a resolution of 5° x 5° x month while for surface gears (purse seine and pole-and-line) the resolution is 1°x 1° x month, excepted for Philippine and Indonesia fisheries. Size frequency data are at a resolution of 5°x 5° (WCPO purse seine) 10°x 20°, or aggregated over a region for the EPO.

Table 6.1: Fisheries definition for bigeye tuna

ID	Gear	Region	Description	Nationality	C/E data month/year	Reso-lution	Size data qtr/year	Reso-lution
L1	LL	WPO 110E-165E 15N-15S	Traditional, BET, YFT target	Japan, Korea, Chinese Taipei (DWFN)	6/1950 - 12/2007	5x5	2/1948 – 1/2007	10x20
L22	LL	CPO 165E-150W 15N-15S	Traditional, BET, YFT target	Japan, Korea, Chinese Taipei (DWFN)	6/1950 - 12/2007	5x5	2/1948 – 1/2007	10x20
L2	LL	10S-45N 110E-140W	Night Shallow	China, Chinese Taipei	1/1958 - 11/2007	5x5	2/1991 – 2/2007	10x20
L3	LL	40S-10S 140E-140W	Albacore target	Chinese Taipei, Vanuatu (DWFN), Korea, Japan	7/1952 - 12/2007	5x5	2/1951 – 4/2006	10x20
L4	LL	40S-10S 145E-140W	Pac. Islands ALB target	US (Am. Sam), Fiji, Samoa, Tonga, NC, FP, Vanuatu (local)	2/1982 - 12/2007	5x5	3/1991 – 4/2007	10x20
L5	LL	20S-15N 140E-175E	Pac. Islands BET, YFT target	PNG, Solomon Is.	10/1981 - 5/2007	5x5	2/1996 – 4/2006	10x20
L6	LL	40S-10S; 140E-175E	Australia East Coast	Australia	10/1985 - 3/2007	5x5	3/1992 – 4/2006	10x20
L7	LL	10S-50N; 130E-140W	Hawaii LL	US (Hawaii)	1/1991 - 12/2006	5x5	4/1992 – 3/2006	10x20
S8	PS	40S-20N; 114E-140W	PS dFAD & log	All	12/1967 - 2/2008	1x1	2/1988 – 3/2007	5x5
S9	PS	40S-20N; 115E-140W	PS aFAD	All	7/1979 - 1/2008	1x1	2/1984 – 2/2007	5x5
S10	PS	40S-20N; 114E-140W	PS School	All	12/1967 - 1/2008	1x1	3/1984 – 3/2007	5x5
S11	PS	10N-50N; 120E-180E	PS Japan domestic	Japan	7/1970 - 8/2007	1x1	-	-
	Misc.	10S-15N; 115E-180E	PH domestic	Philippines	1/1970 - 9/2007	5x5	4/1980 – 4/2007	10x20
	HL	0N-15N; 115E-130E	PH Handline	Philippines	1/1970 - 12/2006 (E missing before 1997)	5x5	1993-2007	10x20
	Misc	10S-10N; 120E-180E	ID domestic	Indonesia	1/1970 - 1/2007 (E partially missing)	5x5	2006	10x20
P15	PL	40S-48N; 115E-140W	Pole-and-line	Japan, Solomon Islands, PNG, Fiji	3/1970 - 12/2006	1x1	2/1965 – 1/2005	10x20
S17	PS	EPO	YFT, Dolphin schools	NA (public data)	1/1959 – 8/2007	1x1	1/1961 – 4/2004	EPO
S17	PS	EPO	YFT, Not associated	NA (public data)	1/1959 – 8/2007	1x1	1/1961 – 4/2004	EPO
S18	PS	EPO	YFT, Floating objects	NA (public data)	2/1959 – 8/2007	1x1	1/1961 – 4/2004	EPO
L23	LL	10N-50N; 150W-90W	Traditional, BET, YFT target	Japan, Korea, Chinese Taipei	11/1954 – 6/2006	5x5	1/1965 – 4/2003	= reg
L24	LL	40S-10N; 150W-70W	Traditional, BET, YFT target	Japan, Korea, Chinese Taipei	10/1954 – 7/2006	5x5	4/1954 – 4/2003	= reg

Optimization experiments

Philippine and Indonesia fishing data are not used in the optimization due to a lack of accuracy.

Bigeye population structure

The structure of the population (Figure 5.1) was defined with 1-month cohort for larvae life stage, two 1-month cohort for juvenile stage, two 2-month and five 3-month cohorts for young fish (before age at maturity) and 11 cohorts for adult stages (three of 4 months, two of 5 months and the last six of 6, 8, 9, 11, 15, and 60 months correspondingly). The last "+ cohort" accumulates older fish. Age at maturity was set to 24 months. Age-length and age-weight relationships are derived from the last MULTIFAN-CL estimate (Davies et al., 2011).

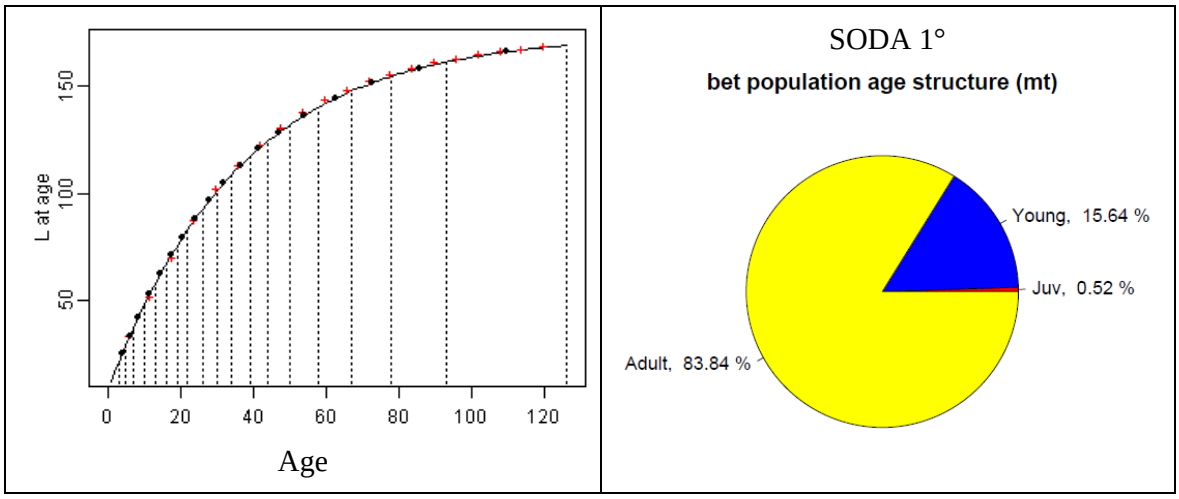

Figure 6.1: Bigeye size (FL in cm) at age (month) and weight (kg) at age functions used in SEAPODYM simulation (left), based on MULTIFAN-CL estimates (Davies et al., 2011), and Population structure (average 1998-2008) in % metric tonnes resulting from the new optimization with SEAPODYM and the SODA-Psat environmental forcing.

Fit to catch data

While the largest catch of bigeye comes from the equatorial band (10°N-10°S), the species habitat ranges between 45°N and 40°S as demonstrated by catch distribution. The overall spatial fit between prediction and observation is provided by the standard R-squared goodness of fit (Figure 6.2). There is a good fit between total observed and predicted catch in the major fishing grounds of the species (Figure 6.3) providing realistic overall fishing mortality. A weak fit is observed in the subtropical gyres where the catch is usually low and the relative error between observed and predicted catch can be larger than 70% in these regions (Figure 6.2:). The fit is also poor in the eastern Pacific between equator and 5°N east of 120°W. The Pearson R-squared provides additional information on the coherence between dynamics of predicted and observed catch (i.e., if their low and high peaks are correlated). The same spatial patterns emerge with this metric however improved fit in the temperate latitude is observed suggesting satisfactory representation of seasonality.

The spatial discrepancies observed originate from several fisheries that can be identified from Figure 5.3. While the model predicted satisfactory fit for all traditional Asian longline fisheries (L1, L2, L23, L24) targeting bigeye and yellowfin tuna, the series for the Pacific islands domestic fisheries (L6) shows a very clear shift before and after the year 2002. Future optimisations would benefit from

investigating the explanation for this shift and should consider splitting the fishery into a pre and post 2002. The predicted CPUE for the western purse seine drifting FAD and log fishery (S8) cannot fit several observed very large peaks, particularly in the second half of 1999, 2000, 2003 and 2005. Similarly a very high variability of observed CPUE cannot be reproduced for the eastern FAD associated purse seine fishery (S18). The fit is much better for the eastern dolphin-associated purse seine fishery (S17) that shows the highest catch rates. Despite the lack of size data, the seasonality in the Japanese water (S11) and the pole and line fisheries (P15) is well predicted.

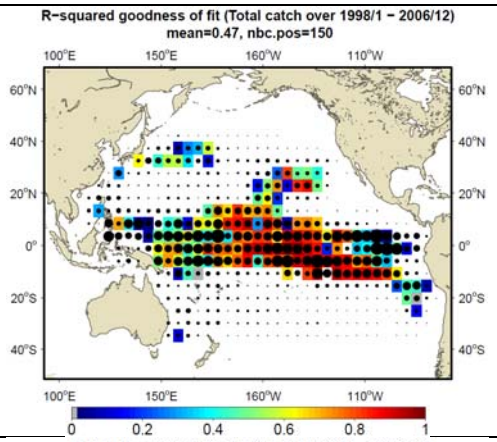

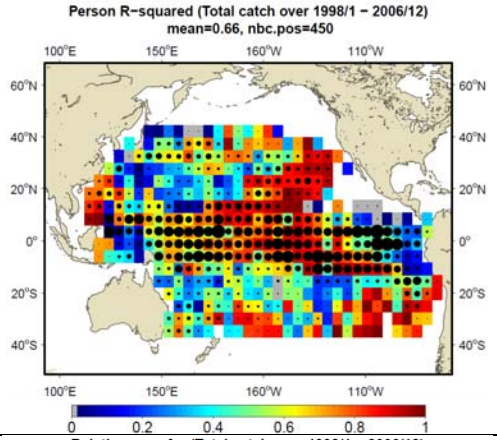

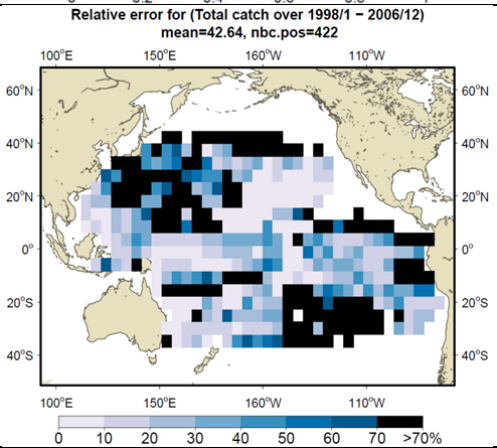

Figure 6.2: Spatial fit to catch data.

Spatial fit for all BET fisheries over the optimization period simulation. Area of circles is proportional to total observed catch. Note that the R-squared goodness of fit is negative in cells where there is nearly zero catch or very frequent null catch events.

Top: Map of R-squared goodness of fit metrics representing the spatial fit over the period used for optimization (white squares indicate negative correlation between observations and predictions), overlaid with the total catch in each cell (black circles proportional to catch)
.
Middle: Map of Pearson r-squared metric, which quantifies the percentage of the catch variance explained by the model in each cell, overlaid with the number of observations (fishing events).

Bottom: Map of the mean error.

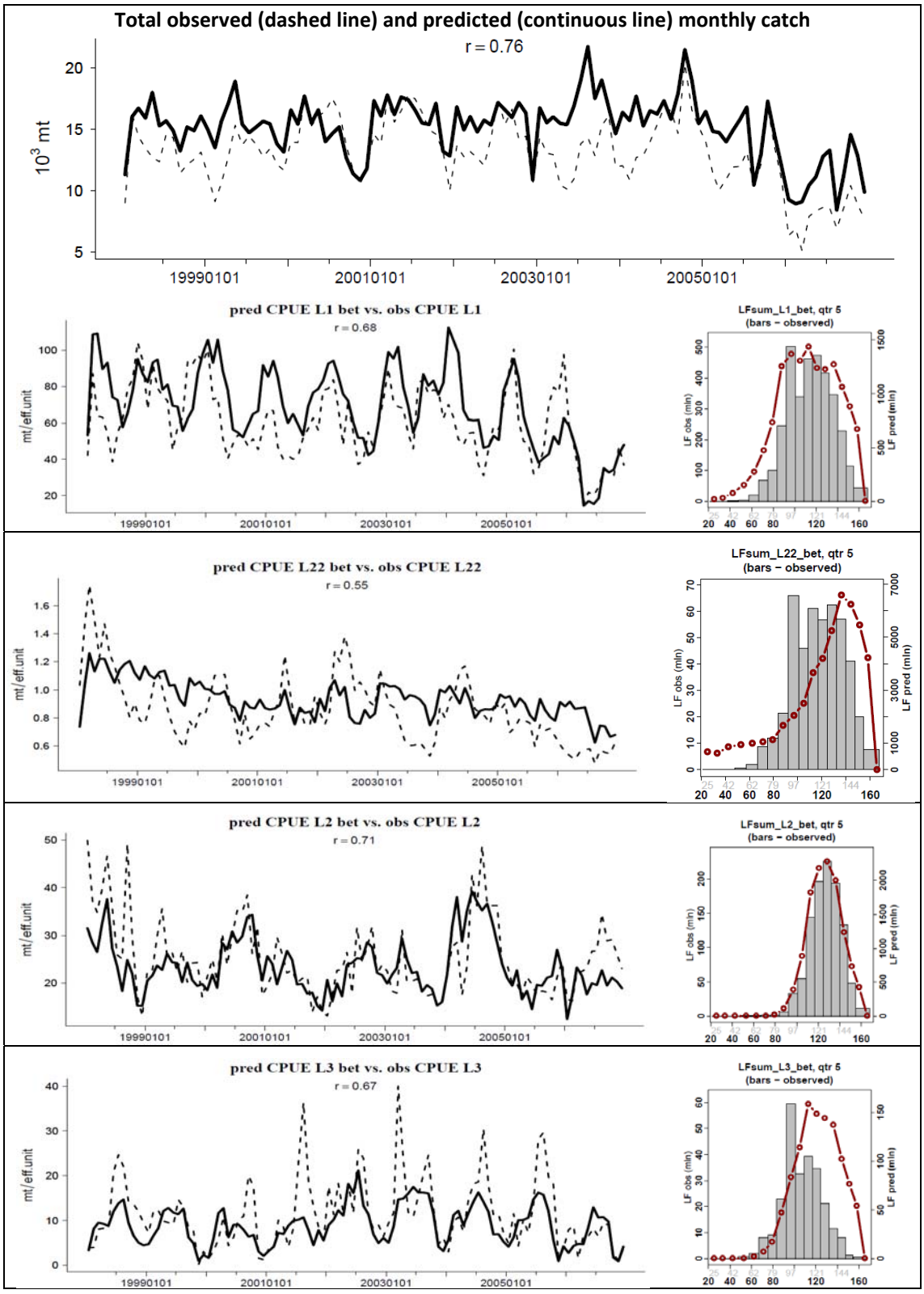
Total observed (dashed line) and predicted (continuous line) monthly catch
r = 0.76
10^3 mt
19990101
20010101
20030101
20050101
pred CPUE L1 bet vs. obs CPUE L1
r = 0.68
mt/eff.unit
LFsum_L1_bet, qtr 5
(bars – observed)
LF obs (mln)
LF pred (mln)
pred CPUE L22 bet vs. obs CPUE L22
r = 0.55
LFsum_L22_bet, qtr 5
pred CPUE L2 bet vs. obs CPUE L2
r = 0.71
LFsum_L2_bet, qtr 5
pred CPUE L3 bet vs. obs CPUE L3
r = 0.67
LFsum_L3_bet, qtr 5

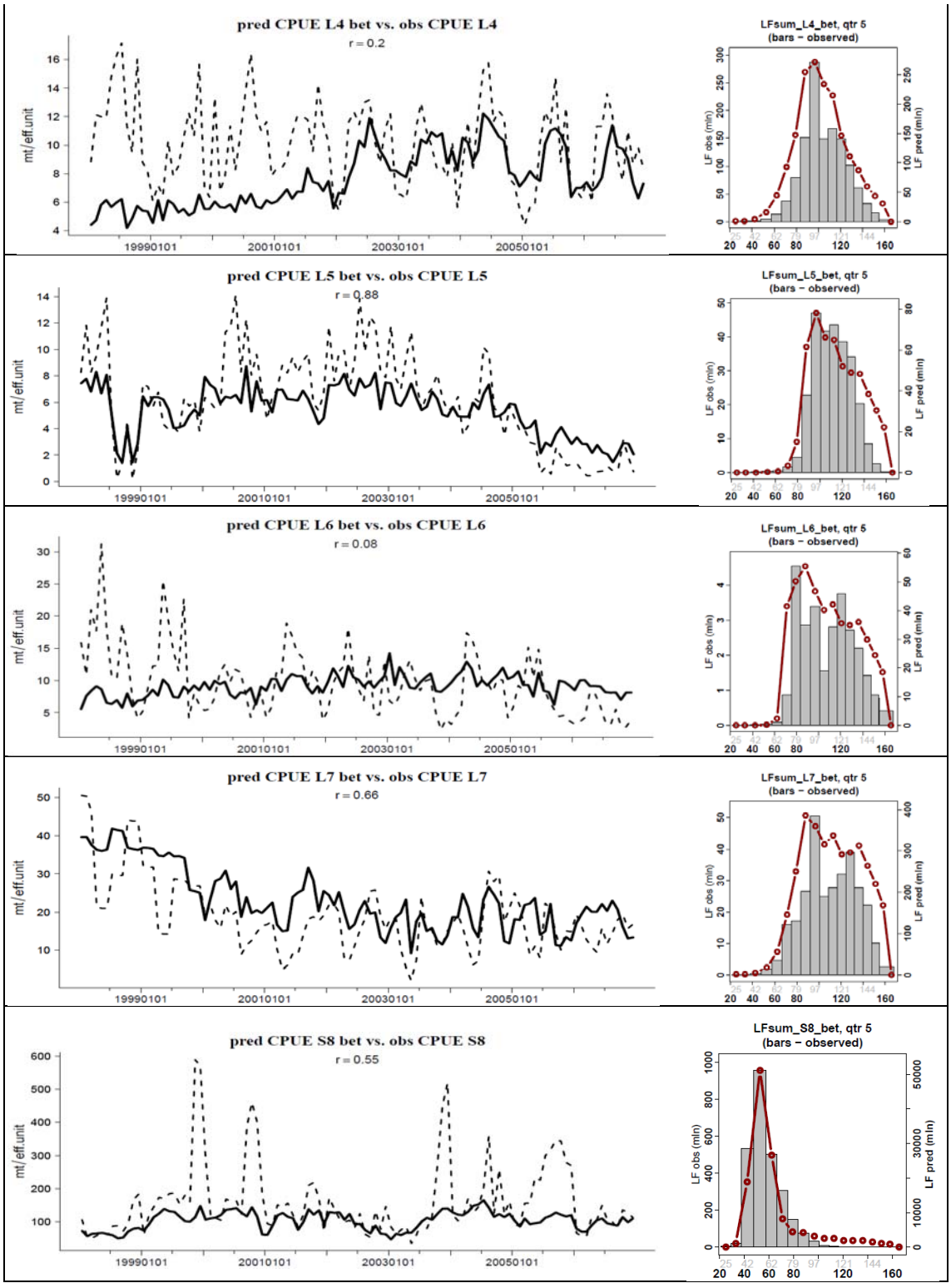
pred CPUE L4 bet vs. obs CPUE L4
r = 0.2
mt/eff.unit
19990101
20010101
20030101
20050101
LFsum_L4_bet, qtr 5
(bars – observed)
LF obs (min)
LF pred (min)
pred CPUE L5 bet vs. obs CPUE L5
r = 0.88
LFsum_L5_bet, qtr 5
(bars – observed)
pred CPUE L6 bet vs. obs CPUE L6
r = 0.08
LFsum_L6_bet, qtr 5
(bars – observed)
pred CPUE L7 bet vs. obs CPUE L7
r = 0.66
LFsum_L7_bet, qtr 5
(bars – observed)
pred CPUE S8 bet vs. obs CPUE S8
r = 0.55
LFsum_S8_bet, qtr 5
(bars – observed)

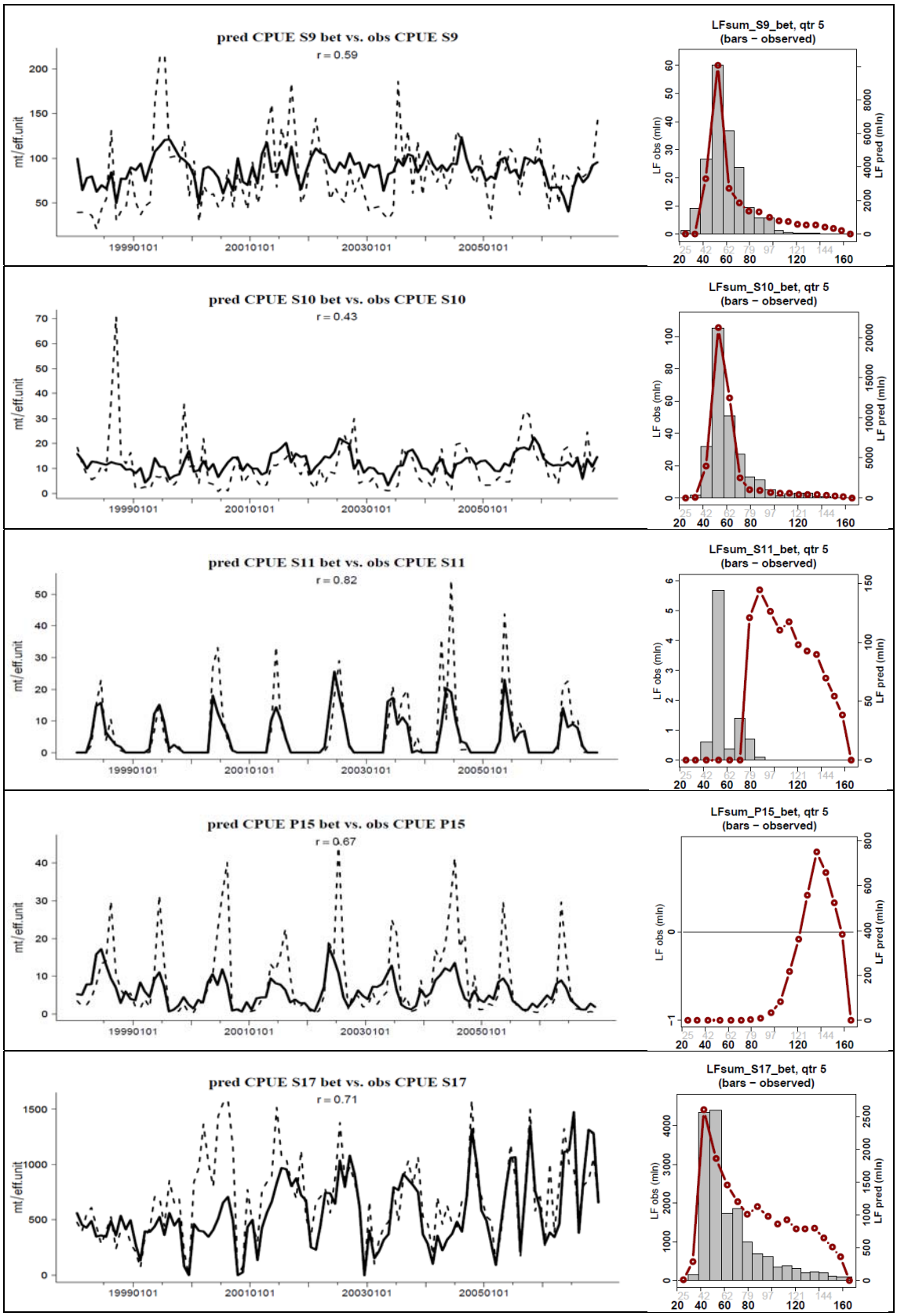
pred CPUE S9 bet vs. obs CPUE S9
r = 0.59
mt/eff.unit
19990101
20010101
20030101
20050101
LFsum_S9_bet, qtr 5
(bars − observed)
LF obs (mln)
LF pred (mln)
pred CPUE S10 bet vs. obs CPUE S10
r = 0.43
LFsum_S10_bet, qtr 5
(bars − observed)
pred CPUE S11 bet vs. obs CPUE S11
r = 0.82
LFsum_S11_bet, qtr 5
(bars − observed)
pred CPUE P15 bet vs. obs CPUE P15
r = 0.67
LFsum_P15_bet, qtr 5
(bars − observed)
pred CPUE S17 bet vs. obs CPUE S17
r = 0.71
LFsum_S17_bet, qtr 5
(bars − observed)

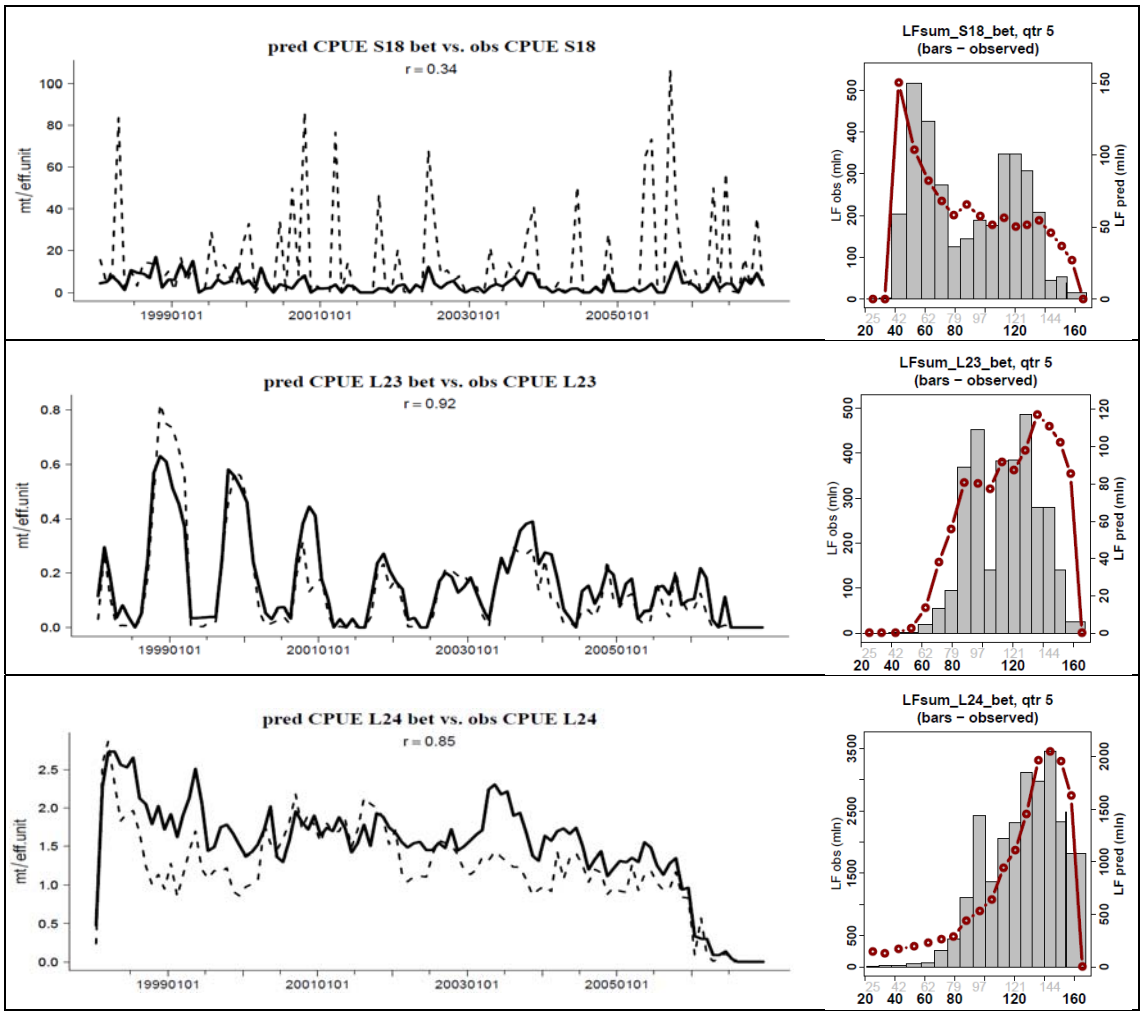

Figure 6.3: Total predicted (continuous line) and observed (dotted line) catch for all fisheries and predicted and observed CPUEs and size frequencies for all fisheries.

Optimal Parameterization

The optimization was not able to correctly estimate some of parameters for habitat and movements (Table 6.2). The standard error of the spawning temperature function and the diffusion parameter were fixed. The standard error of the adult temperature function at maximum age was estimated near its lower boundary.

Natural mortality

The resulting average mortality rates (weighted by the cohort density) gives values rapidly decreasing from above 0.6 mo^{-1} for the first (larvae) cohort to less than 0.1 mo^{-1} for cohorts older than 1.5 year (Figure 6.4).

Spawning and larval recruitment

Optimal spawning temperature (SST) was estimated to 28.29 °C with standard error being fixed to 1°C. This resulted in a predicted distribution of larvae with maximum abundance between 27 and 29°C (Figure 6.5). The seasonal timing of spawning migration estimated with the SODA 1° configuration is quite different from the previous one achieved with NCEP-ORCA2 (Figure 6.6). In this latter simulation based on a long time series of data, the seasonal switch peaked near the spring

equinox and was effective above latitude 13°. In the new simulation with SODA, the peak occurs much later and impacts fish only in latitude higher than 34°. It is likely that the shorter time series for this new configuration does not allow a good estimate of these parameters. This is certainly one feature that will need to be examined in future optimization experiments.

Table 6.2: Estimates of habitats and movement parameters of previous simulations and the new one using environmental forcings from SODA and IPSL-CM4 before and after correction of temperature fields.

Parameters estimated by the model			**Unit**	**NCEP-ORCA2**	**SODA**
T_s	Spawning	Optimum of the spawning temperature function	°C	26.13	28.29
σ_s		Std. Err. of the spawning temperature function	°C	2*	1*
α		Larvae food-predator trade-off coefficient	-	0.33	4.93
T_a	Feeding habitat	Optimum of the adult temperature function at maximum age	°C	[6.5	[8
σ_a		Std. Err. of the adult temperature function at maximum age	°C	4.5]	2.8
$\hat{O}$		Oxygen threshold value at Ψ_O =0.5	$mL \cdot L^{-1}$	0.89	0.61
D_{max}	Move-ment	Diffusion parameter		0.06*	0.02*
V_{max}		Maximum sustainable speed	$B.L.\ s^{-1}$	0.834	0.32

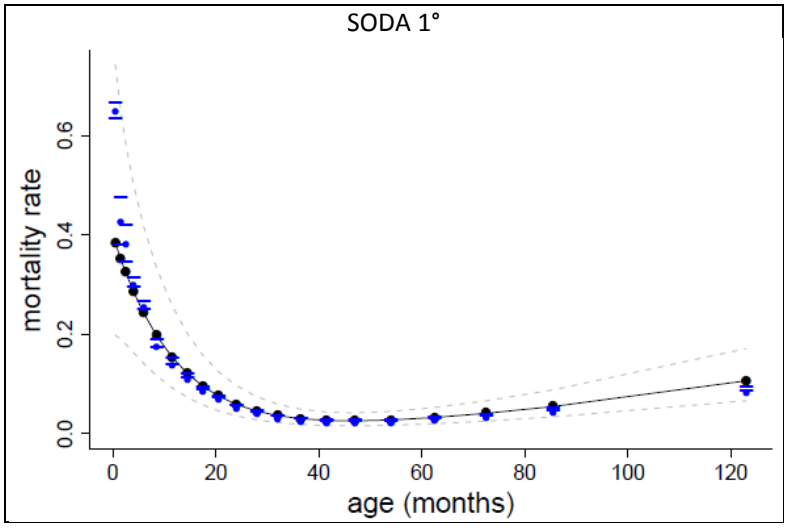

Figure 6.4: Natural mortality rates ($month^{-1}$) estimated from SEAPODYM optimization experiments. Black dotted line corresponds to the theoretical average mortality curve whereas blue dots indicate the mean mortality rates weighted by the cohort density.

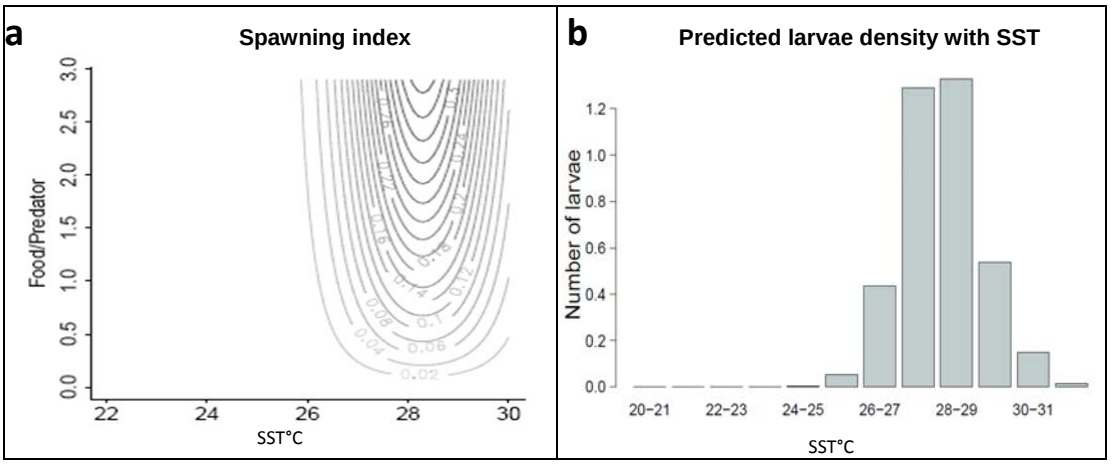

Figure 6.5: Spawning and larval recruitment. **a)** Spawning index in relation to SST and food-predator tradeoff ratio and **b)** Distribution of larvae according to SST and the estimated parameters of spawning index.

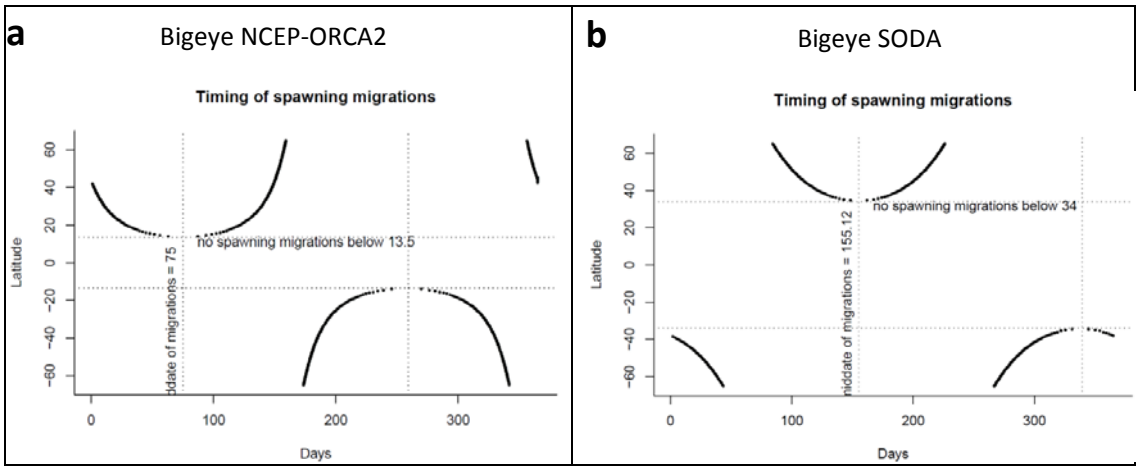

Figure 6.6: Seasonal timing of spawning migration estimated with a) NCEP-ORCA2 hindcast and b) SODA 1°.

Feeding habitat

The optimal value for the oldest cohort was estimated systematically at the lower boundary 8.0 °C but the standard error was estimated. The threshold value for the oxygen tolerance was estimated 0.61 ml/l (Figure 6.7), slightly lower than in previous experiment. However it should be noted that the SODA configuration using primary production derived from satellite data is relying on a monthly climatology of dissolved oxygen concentration, i.e., without interannual variability, rather than on a prognostic variable estimated by a biogeochemical model as in the case of NCEP-ORCA2.

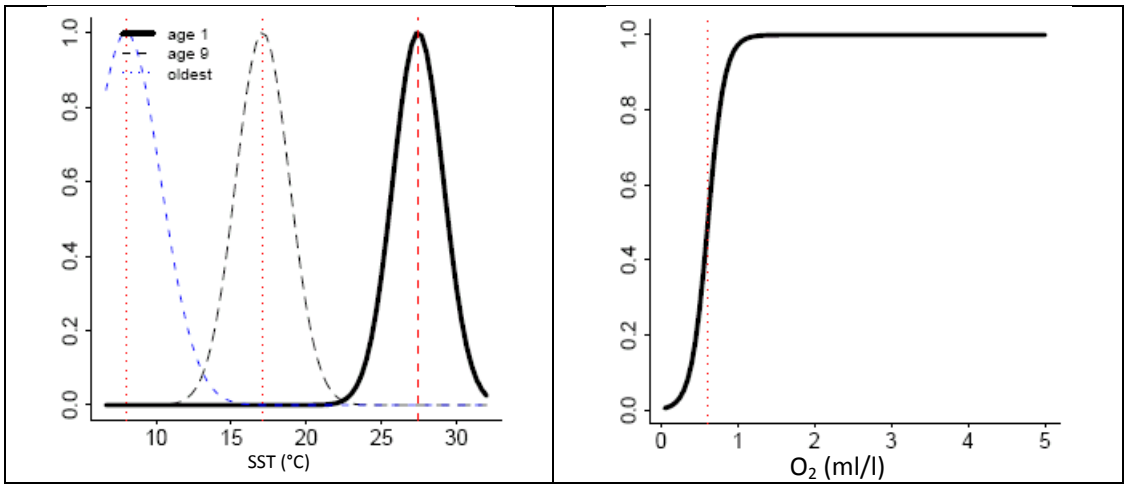

Figure 6.7: Bigeye - Optimized functions for temperature and oxygen habitats.

Movements

The value for maximum sustainable speed was estimated to 0.32 Body Length/s, but the diffusion coefficient for fish movements had to be fixed (Figure 6.8). The maximum diffusion rates weighted by cohort density remain below 600 nmi^2 $month^{-1}$ and the mean of maximum sustainable speed decreases exponentially with age (size). It remains below 0.05 BL/s for fish older (larger) than 2 years (80 cm). The decreasing trend with size can be attributed to an increasing accessibility with age (size) to forage biomass of deeper layers, thus decreasing the horizontal gradients of the feeding habitat index controlling the movement. These gradients are still smaller than for skipjack since bigeye has less constraint to access deepest layer characterized by cold temperature and low oxygen concentration.

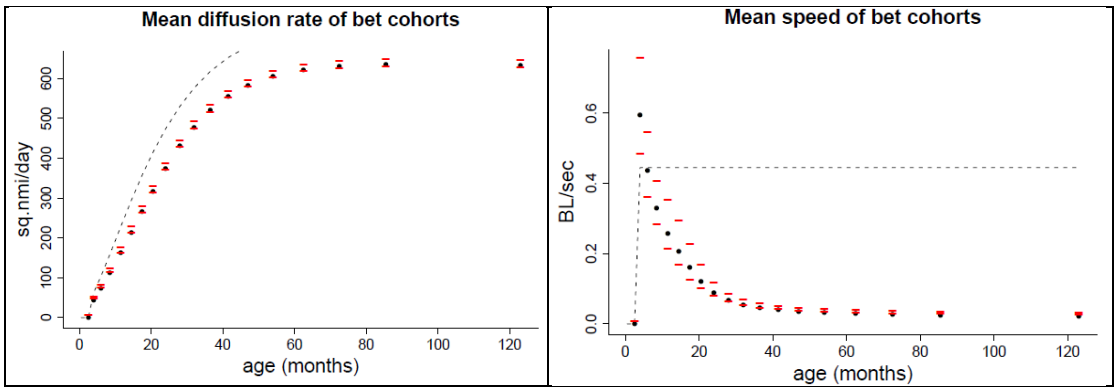

Figure 6.8: Maximum speed and diffusion rates by cohort (depending of age/size and habitat value / gradient) based on SEAPODYM parameterization (dotted lines) and predicted means weighted by the cohort density (black dots) with one standard error (red bars).

Biomass estimates and population dynamics

The total biomass estimates (Figure 6.9) are presented with those estimated from the previous 2° x month optimisation using (NCEP-ORCA2-PISCES with the initial conditions of the SEAPODYM simulation starting in 1977). The estimate is approximately 40% higher than these alternate values.

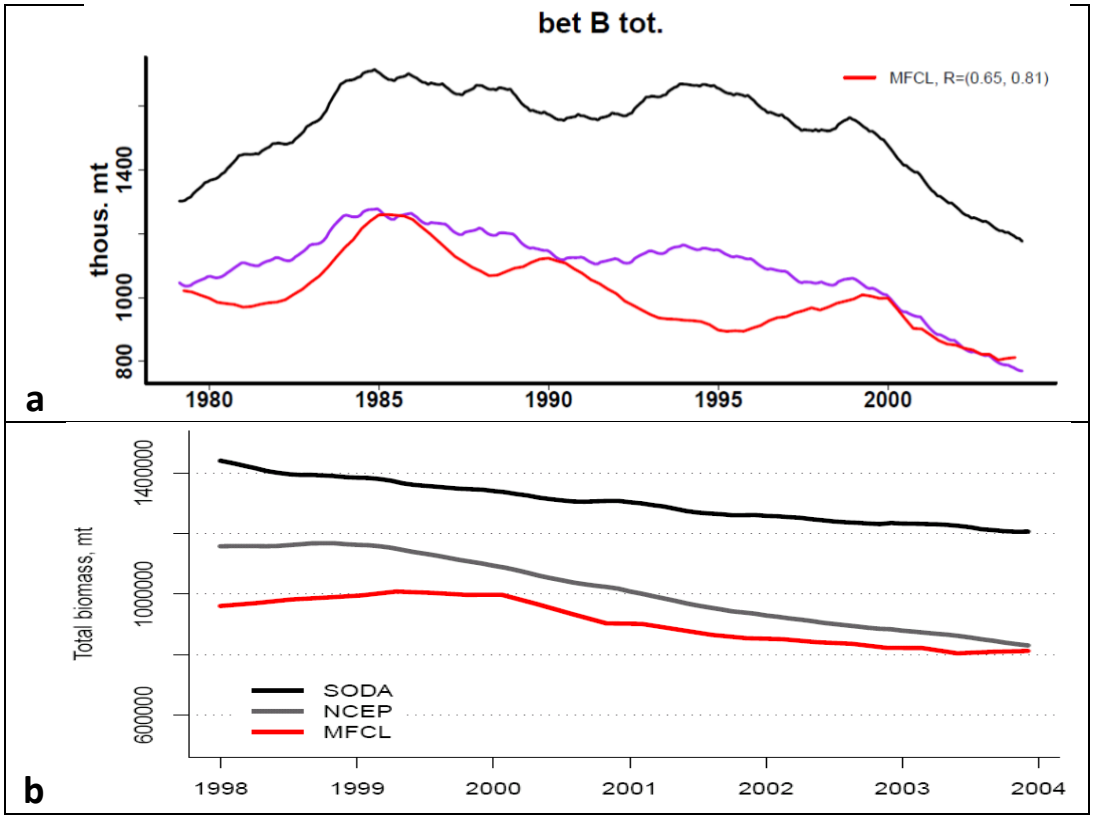

Figure 6.9: Estimates of total Pacific biomass of bigeye: **a**) with stock assessment model MULTIFAN-CL (red) and SEAPODYM -NCEP 2° configuration using no constraint (black) or initial conditions provided by MUTIFAN-CL (purple) and **b**) with the new estimate using SODA 1° configuration (black) compared to stock assessment model MULTIFAN-CL (red) and SEAPODYM NCEP 2° configuration with initial conditions provided by MUTIFAN-CL (grey).

The mean spatial distribution (Figure 6.10) shows the highest concentration to be in the central-eastern equatorial region extending east to the coast of Central America. Secondary areas with lower density of bigeye occur in the South west Pacific, especially the Coral Sea, off the coast of Mexico and Baja California and in the North-east off the coast of Philippines islands and south of Japan.

Seasonality in the biomass of adult fish was not estimated (Figure 6.11). The predicted spawning grounds and highest larvae concentration occur in the central and eastern equatorial region (Figure 6.12) with a seasonal peak in the central area during the 3rd quarter. In the Coral Sea, a north-south spatial shift is predicted likely in relation with the seasonal warming of waters; the most southern extension occurring during the austral summer (Q1). The first quarter was the most favourable season for spawning in the north-western quadrant of the basin, with the highest density off the Philippines. The young immature fish are particularly concentrated in the central equatorial region (Figure 6.13).

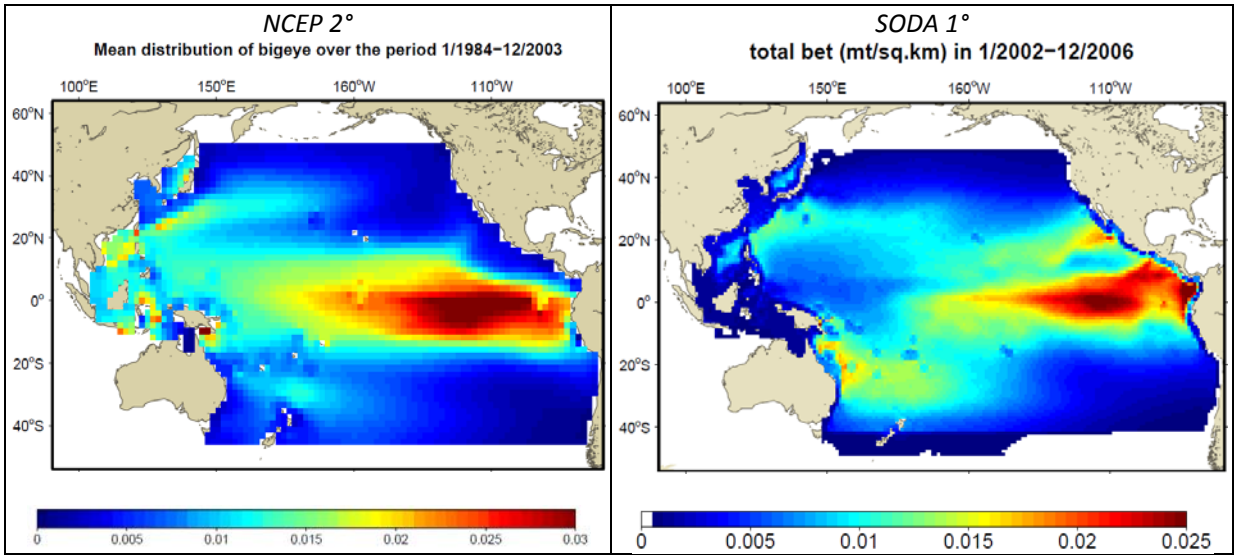

Figure 6.10: Predicted total biomass of Pacific bigeye, average over 2002-2006.

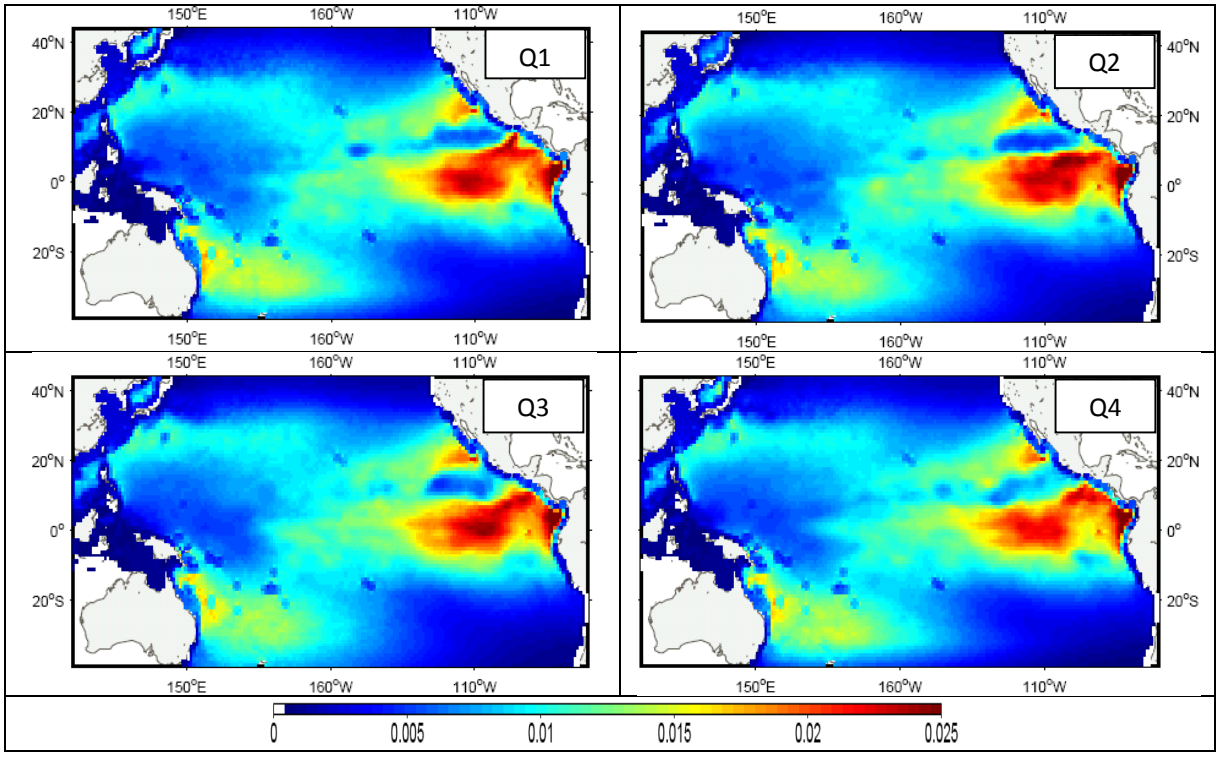

Figure 6.11: Seasonal distributions of adult bigeye, average over 2002-2006 years.

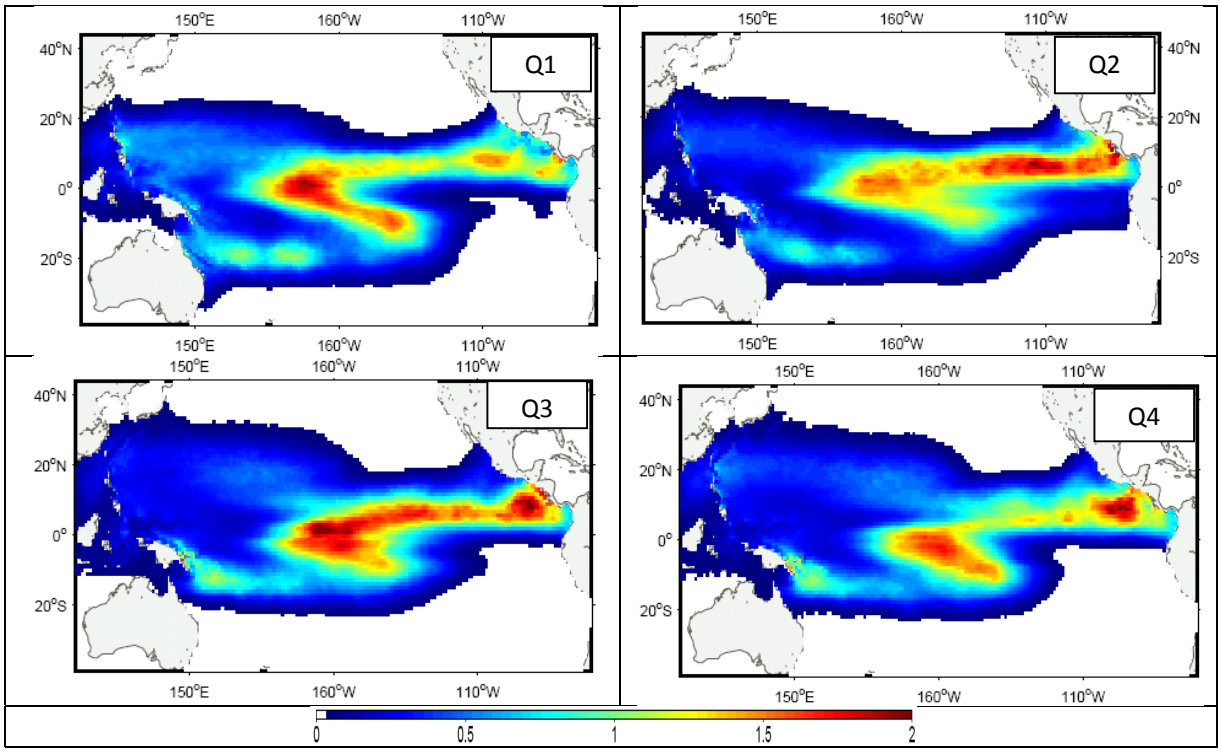

Figure 6.12: Seasonal distributions of bigeye larvae, average over 2002-2006 years.

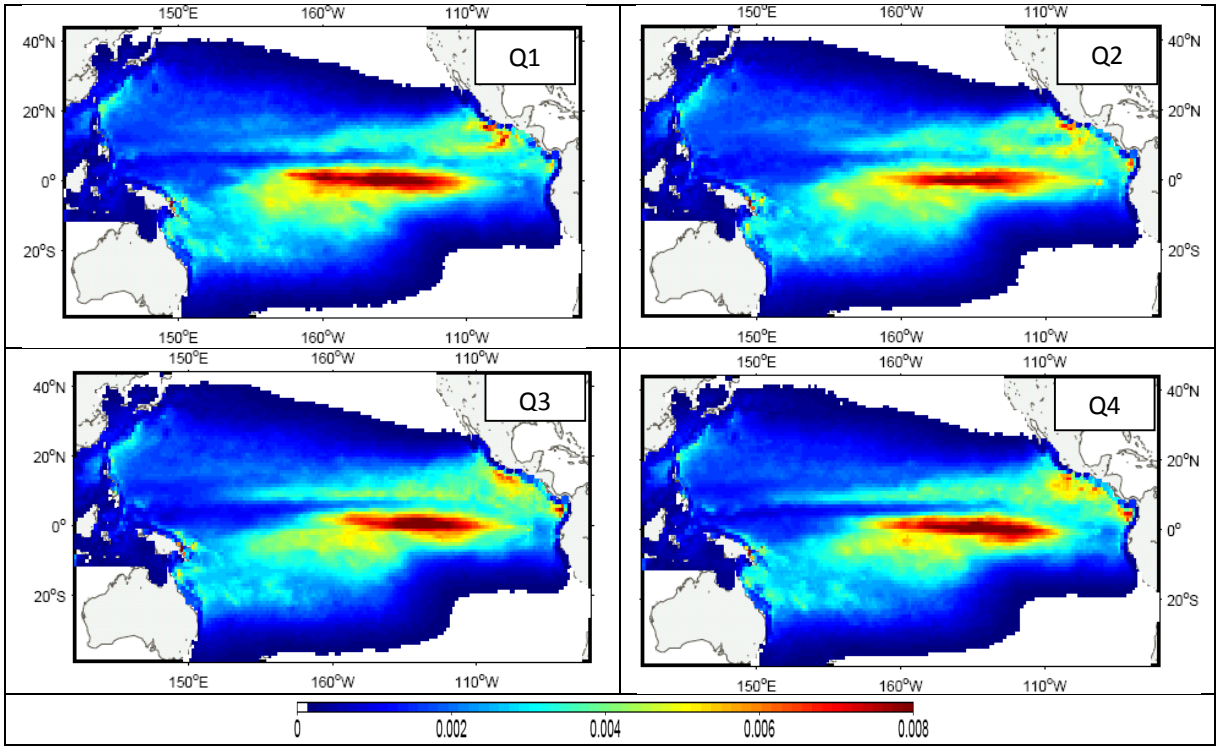

Figure 6.13: Seasonal distributions of young bigeye, average over 2002-2006 years.

7. REFERENCE FIT FOR SOUTH PACIFIC ALBACORE FOR THE HISTORICAL PERIOD (SPALB1.1 NCEP-ORCA2-v2)

Physical forcing: NCEP-ORCA2-PISCES hindcast simulation (1958-2003)

In absence of historical synoptic datasets for oceanic physical variables before the 1980s, and before 1998 for the ocean color (i.e., SeaWiFS), ocean reanalyses are not available to simulate tuna dynamics with SEAPODYM for the past decades before 1998. As an alternative, hindcast simulations with coupled ocean physical-biogeochemical models can be used. These simulations are forced by atmospheric data for which a few reanalyses are available (e.g. NCEP, ERA40). To produce the first initial conditions used in optimization experiments with the reference configuration, or to run specific applications requiring long historical simulations, one such hindcast is used to drive the model SEAPODYM. The biogeochemical model is PISCES (Pelagic Interaction Scheme for Carbon and Ecosystem Studies; Aumont and Bopp, 2006). It incorporates both multi-nutrient limitation (NO3, NH_4, PO_4, SiO_3 and Fe) and a description of the plankton community structure with four plankton functional groups (Diatoms, Nano-phytoplankton, Micro-zooplankton and Meso-zooplankton). PISCES is coupled to the ORCA2 configuration of the ocean circulation model OPA (http://www.nemo-ocean.eu/), and driven by the NCEP-NCAR reanalysis, that provides 50-year record of global analyses of atmospheric fields based on the recovery of land surface, ship, rawinsonde, pibal, aircraft, satellite, and other data. (http://www.cgd.ucar.edu/cas/guide/Data/ncep-ncar_reanalysis.html). This hindcast simulates reasonable seasonal, interannual and decadal variability at basin-scale at a coarse resolution of 2°x2°x month.

Fishing data

The definition of fisheries for south Pacific albacore tuna (Table 9.1) was slightly modified from the previous one used for SCIFISH project. The Japanese longline fishery was divided into two fisheries based on the geographical fishing ground, i.e., either tropical (Equator to 25°S) or temperate (25°S-50°S). Further, the island fisheries, previously groupped into a single fishery, were separated. All longline catch and effort fishing data are at a solution of 5° x 5° x month. Size frequency data are at a resolution varying from 5°x 5° to 10°x 20°.

Discussions with colleagues at SPC concerning a possible upgrade of fishing data to enhance spatial resolution at 1°x1° led to a new definition of fisheries that should include one set of incomplete high resolution (1°x month) and one set of complete but low resolution data. Part of these new data sets was provided but it is still too partial to be used in optimization.

Table 7.1: Fisheries definition for south Pacific albacore

N	Gear	Region	Description	Nationality	C/E data month/year	Reso-lution	Size data qtr/year	Reso-lution
(L1) L1	LL	50S-25S; 140E-110W	JP, JPDW	Japan high latitude	1/1952-12/2006	5x5	3/1964-3/2005	10x20
(L1) L12	LL	25S-0; 140E-110W	JP, JPDW	Japan low latitude	1/1952-12/2006	5x5	3/1964-3/2005	10x20
L2	LL	50S-0; 140E-110W		Korea	3/1962-12/2008	5x5	1/1966-2/2006	5x5
L3	LL	50S-0; 140E-110W	Distant-water fleet	Chinese Taipei	7/1964-12/2008	5x5	3/1964-2/2007	5x5; 10x20
L4	LL	50S-10S; 140E-175E	LL targeting Alb	Australia	3/1985-12/2007	5x5	2/2002-2/2007	5x5; 10x20
L5	LL	25S-0; 150E-180E	LL targeting Alb	New Caledonia	11/1983-12/2007	5x5	1/1993-4/2007	5x5; 10x20
L5	LL	25S-5S; 180E-140W	LL targeting Alb	Tonga	2/1982-3/2008	5x5	3/1995-242006	5x5; 10x20
L5	LL	25S-0; 180E-110W	LL targeting Alb	French Polynesia	1/1992-5/2007	5x5	2/1991-4/2007	5x5; 10x20
(L5) L11	LL	25S-0; 180E-155W	LL targeting Alb	American Samoa, Samoa	1/1993-5/2008	5x5	1/1998-3/2007	5x5; 10x20
L6	LL	50S-0; 140E-180W	LL targeting Alb	Other	11/1957-12/2008	5x5	3/1963-3/2005	5x5; 10x20
L7	LL	50S-25S; 145E-180E	LL targeting Alb	New Zealand	8/1989-12/2007	5x5	2/1992-4/2006	5x5; 10x20
L5	LL	25S-0; 150E-180E	LL targeting Alb	Fiji	8/1989-12/2007	5x5	3/1992-3/2007	5x5; 10x20
T8	T	50S-25S; 140E-110W	Troll	New Zealand, United States	1/1967-12/2007	5x5	4/1986-2/2006	5x5; 5x10; 10x20
G9	D	45S-25S; 140E-125W	Driftnet	Japan, Chinese Taipei	11/1983-1/1991	5x5	4/1988-1/1990	5x5; 10x20
L10	LL	50S-0; 180-70W	LL targeting Alb	Other	11/1957-12/2008	5x5	3/1963-3/2005	5x5; 10x20

Optimization experiments

The first likelihood optimization for south Pacific albacore was performed with a first NCEP-ORCA2-PISCES ocean hindcast simulation over the period 1980-2001 (SCIFISH project). Outputs from this first experiment were used for defining initial conditions of a second optimization experiment using SODA ocean reanalysis and satellite derived primary production at 1°x month resolution over the period 1998-2008.

This third optimization experiment uses a new definition of fisheries (cf above) and an updated NCEP-ORCA2-PISCES forcing (1958-2008). It was conducted over the period 1975-2000, with the revised fine age-structure.

South Pacific albacore population structure

The structure of the population was defined with 1-month cohorts for all life stages. Such fine age structure has been chosen to match the time stepping for the integration of the model equations. The last "+ cohort" accumulates older fish. Age at maturity is thus set to 53.5 months. Age-length and age-weight relationships (Figure 7.1) are derived from the last MULTIFAN-CL estimate (Hoyle et al. 2012).

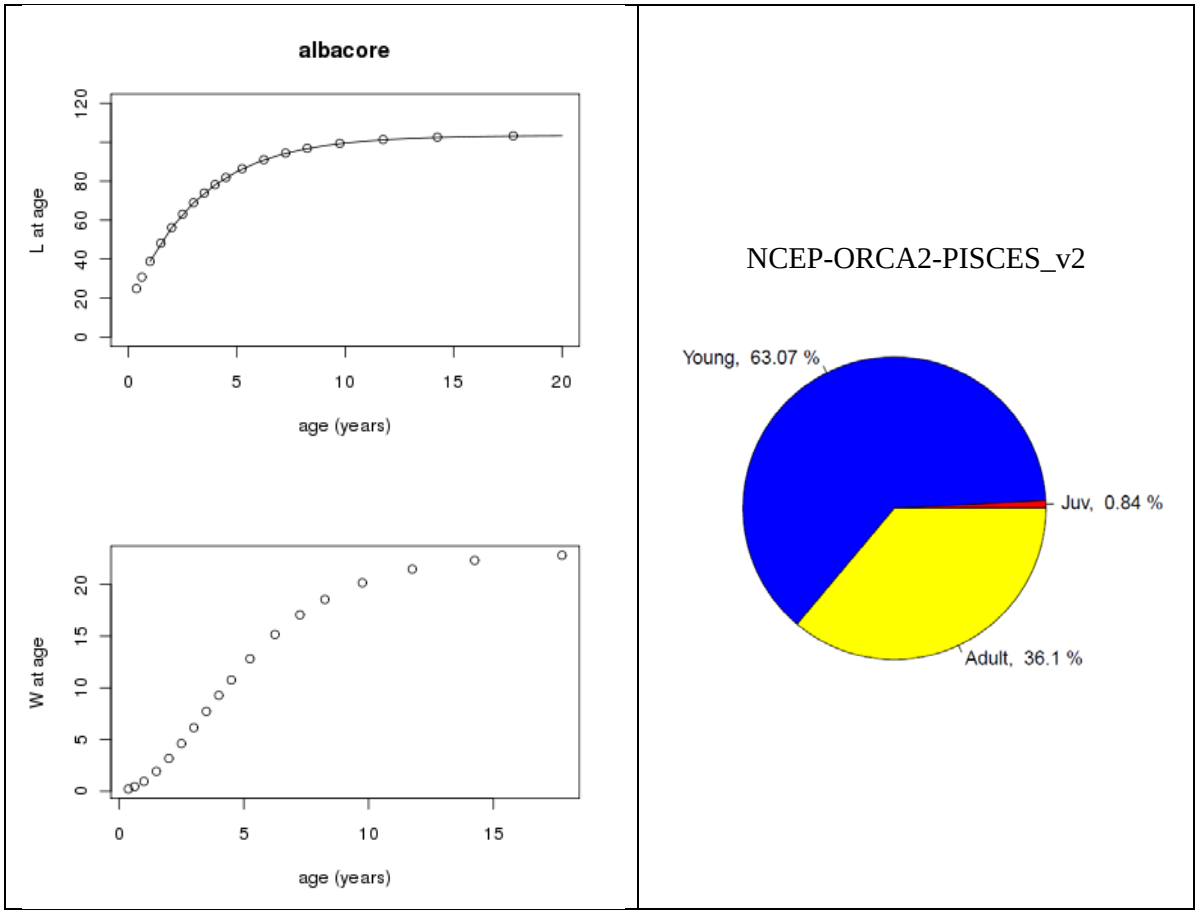

Figure 7.1: South pacific size (FL in cm) at age (month) and weight (kg) at age functions used in SEAPODYM simulation (left), based on MULTIFAN-CL estimates (Hoyle et al 2012), and population structure (average 1998-2008) in % metric tonnes resulting from the new optimization with SEAPODYM and the SODA-Psat environmental forcing.

Fit to catch data

The south Pacific albacore habitat extends between the equator and 45°S (Figure 7.2). The maximum amount of catch occurs in the 10°S-20°S latitudinal band and catch levels are also higher in the west than in the east. There is almost no catch in the eastern equatorial Pacific, likely in relation to the hypoxic waters that characterize the sub-surface layer of this region. The overall spatial fit between prediction and observation is provided in Figure 7.2. The fit between the southern limit of the species habitat and 10°S was good but degraded in the band 10°S - 0°. The total catch in this area however was generally well predicted (Figure 7.3). Dissolved oxygen concentration in the equatorial

region is closely linked to primary productivity and varies strongly with ENSO events. The lack of interannual variability for the oxygen variable may be the reason for the poor fit, especially the Pearson r- squared, in this area with this configuration.

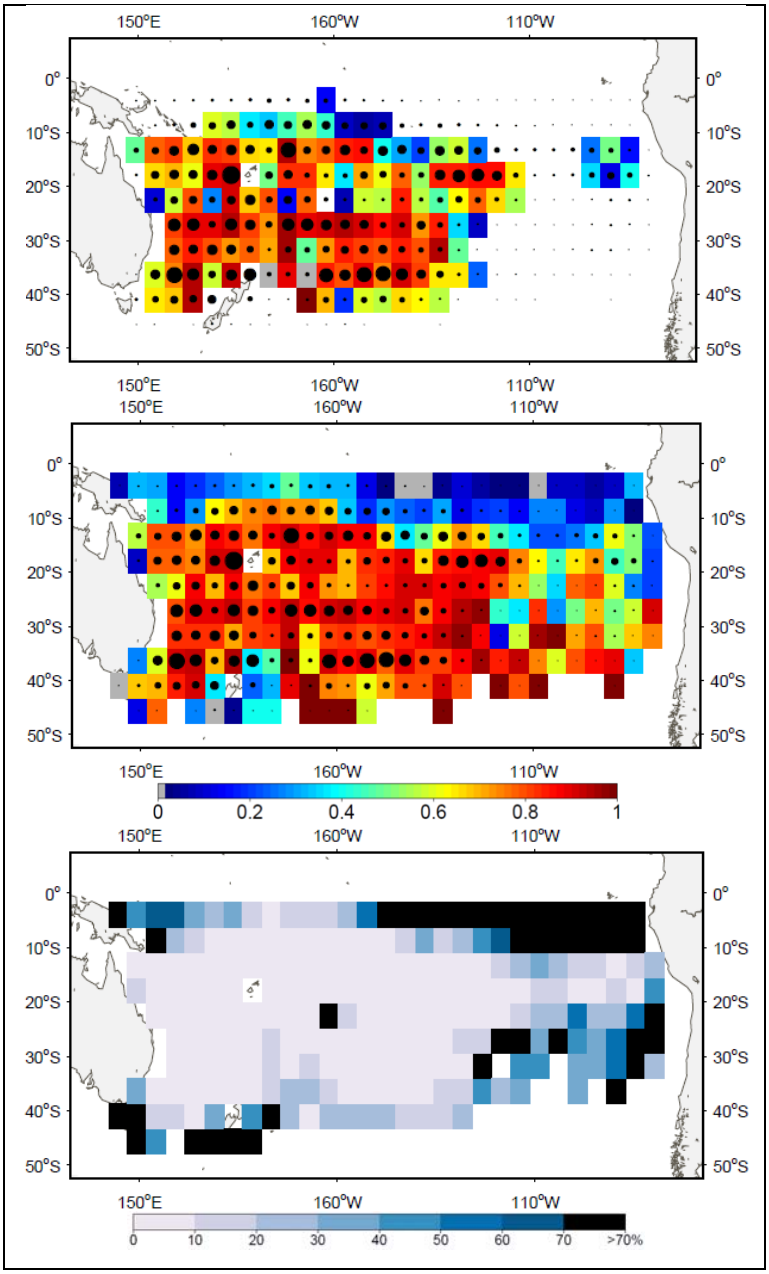

Figure 7.2: Spatial fit to catch data. From top to bottom: 1) Map of R-squared goodness of fit in 5deg cell (mean value 0.68). The cells without color mean no significant fit has been achieved for these usually accidental data. 2) Pearson r-squared metric (mean value 0.78), which quantifies the percentage of the catch variance explained by the model in each cell, overlaid with the number of observations (fishing events). 3) Map of the mean relative error.

The fisheries that show the lowest fit between observed and predicted CPUE are mainly the domestic fisheries (Tonga, Wallis and Futuna, Samoa, Australia). The use of fishing data at 1°x month resolution for these fisheries could help to improve the model skills. The quality of Japanese fishery CPUE (L1 and L12) was poor fact due to the lack of fit in the tropical and transition zones. However, in the sub-tropical (presumably feeding) zones it was good. Comparison of climatological time series of predicted vs observed variables shows reasonable fit for the largest albacore fisheries.

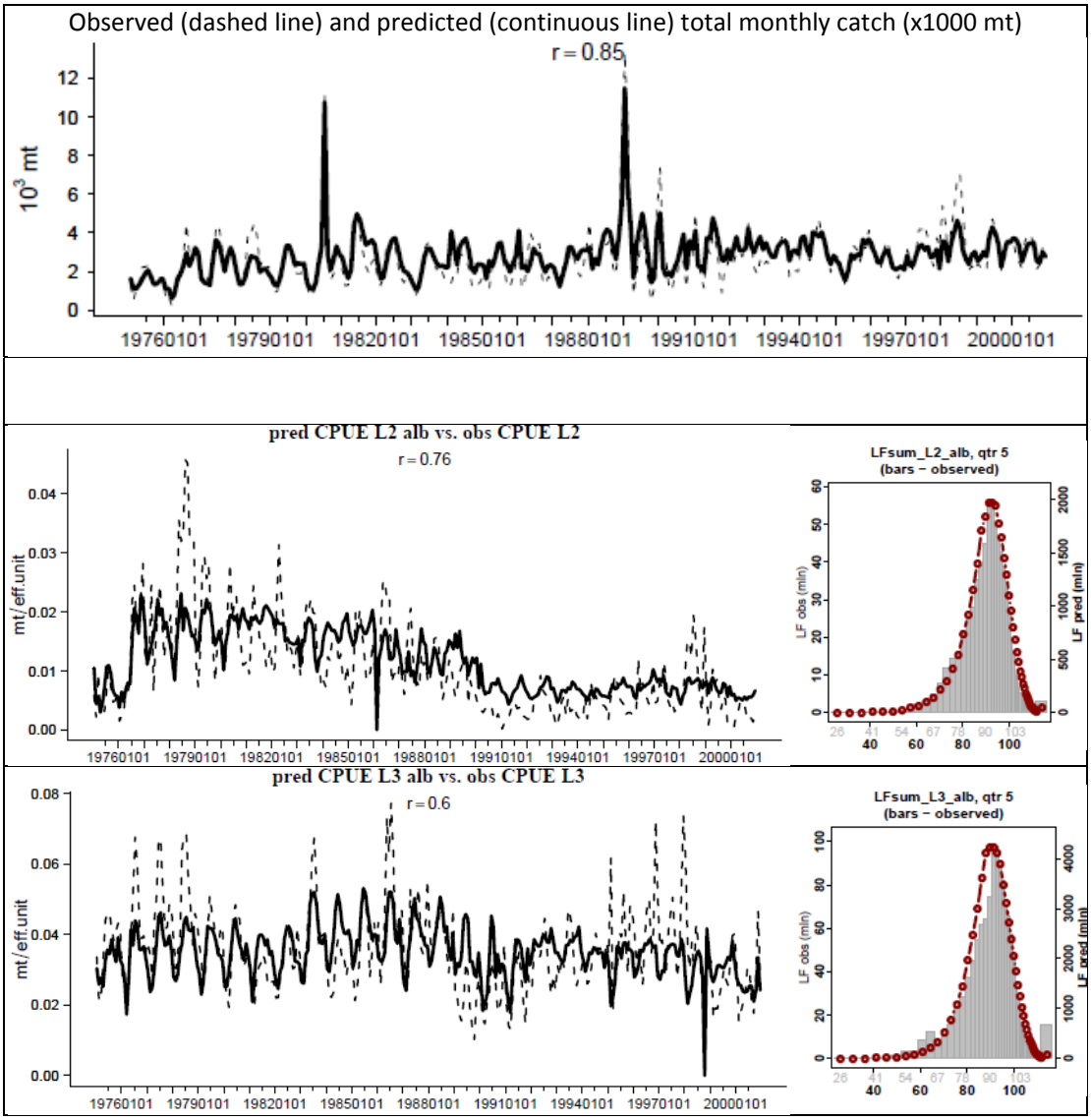

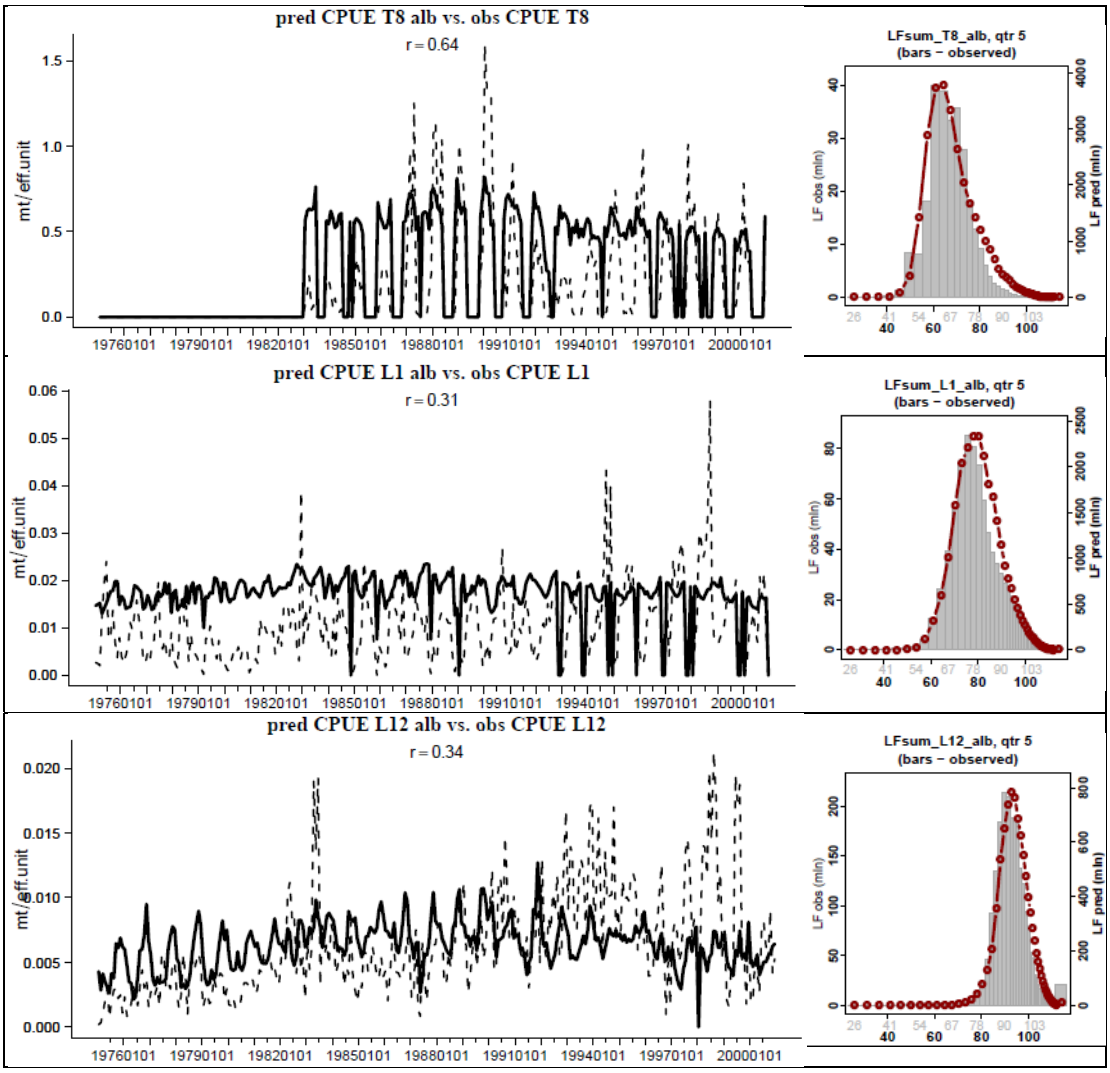

Figure 7.3: Time series of total predicted and observed catch and CPUE by main albacore fisheries (dashed line - observations, solid line - model predictions) with corresponding size frequency for all the domain and time period (bars: observations, red line: model predictions).

Additional model validation was done within specific geographic zones, where the fishing data show the greatest seasonality, assumingly linked to albacore migration cycle. Thus, several regions (Figure 7.4) were chosen with regions R1 and R2 (separated by longitude 180°E) representing known spawning zone; R3 (between 25S and 35S) a transition zone ; R4 (below 35S) the feeding WCPO zone and two EPO zones (R5 and R6) split at 115W.

Figures 7.5 to 7.7 provide the seasonal fit (average over 1975-2000) in these regions for the main longline fisheries, i.e., Japan and Chinese Taipei fleets. Observed and predicted monthly total catch and average CPUE are shown with the total exploited biomass, i.e., the total biomass caught if the catchability was equal to 1. It is calculated as the total biomass multiplied by the selectivity for cell where there is effort.

The fit is very good for the Chinese Taipei fleet (L3) in all regions, and less good for the Japanese fleets, especially the tropical fleet (L12) that progressively focused on bigeye tuna and catch albacore more and more as a by-catch. Based on L1 and L3, the seasonality in spawning grounds R1 and R2 is marked by a high peak in the last quarter and a low peak between March and June (Figure 7.5). During this latter period a high peak occurs in the feeding region R4 and transition region R3 (Figure 7.6). The two eastern regions R5 and R6 have quite different seasonal patterns (Figure 7.7), with a high peak between March and May in the most eastern (R6) and during the last quarter in region R5, ie coinciding with those of spawning region R1 and R2. These complex dynamics may reflect two different migration paths, e.g. north-south in the Coral Sea and west Pacific and following the border of the gyre in the east.

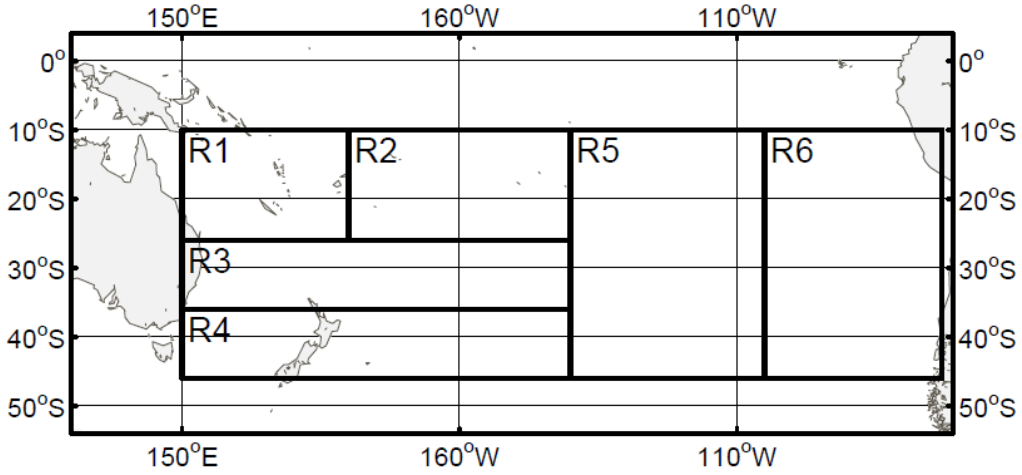

Figure 7.4: Regions used to compare seasonal dynamics of predicted and observed statistics for albacore

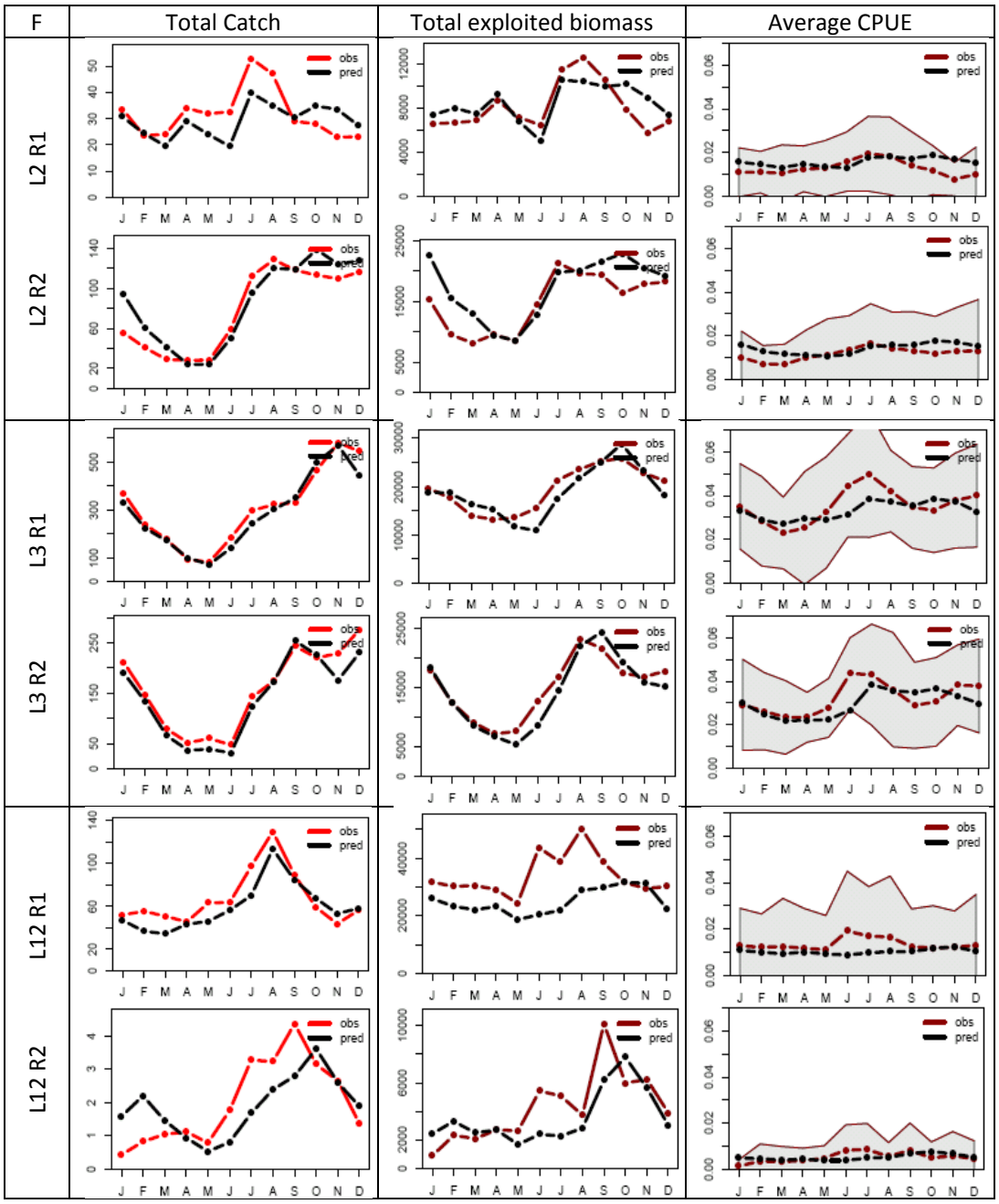

Figure 7.5: Monthly climatology of model predictions vs. observations in two spawning zones (see map on Fig. 8.4). Shaded zone in average CPUE series corresponds to 95% CI.

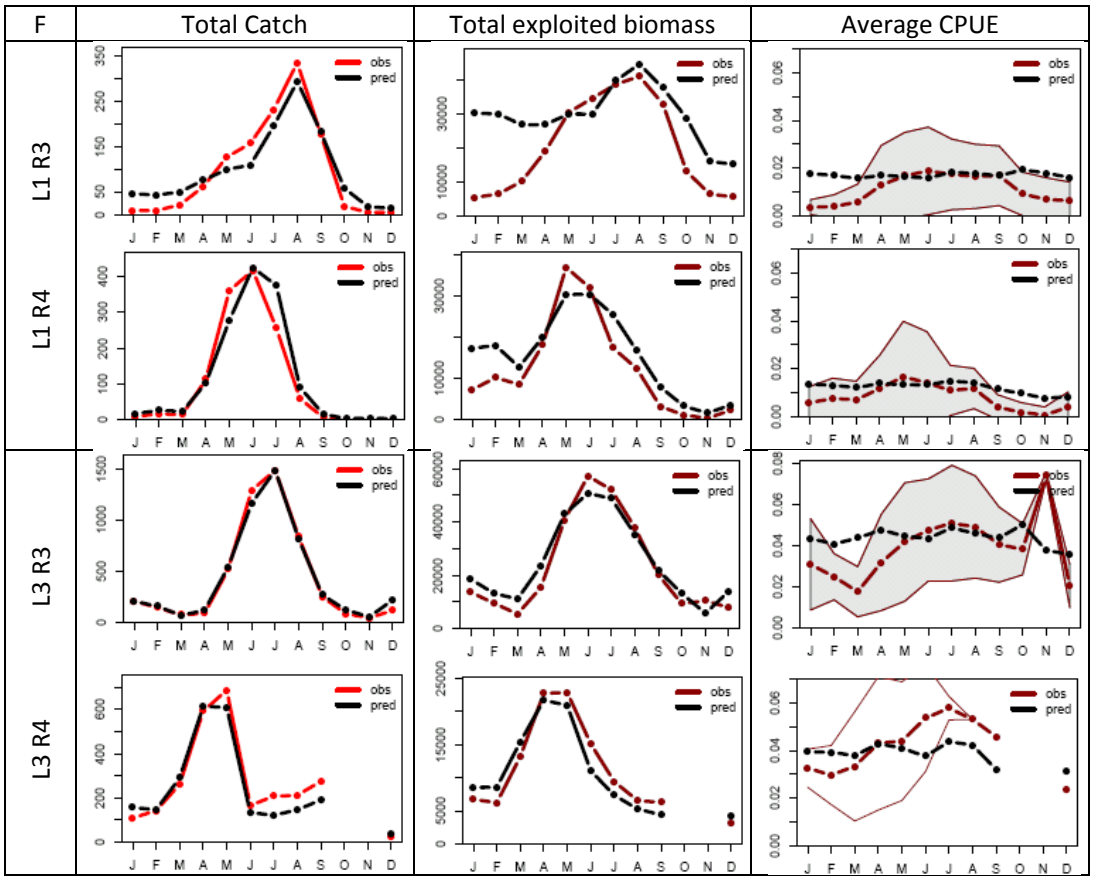

Figure 7.6: Monthly climatology of model predictions vs. observations in WCPO transition and feeding zones (see map on Fig. 8.4). Shaded zone in average CPUE series corresponds to 95% CI.

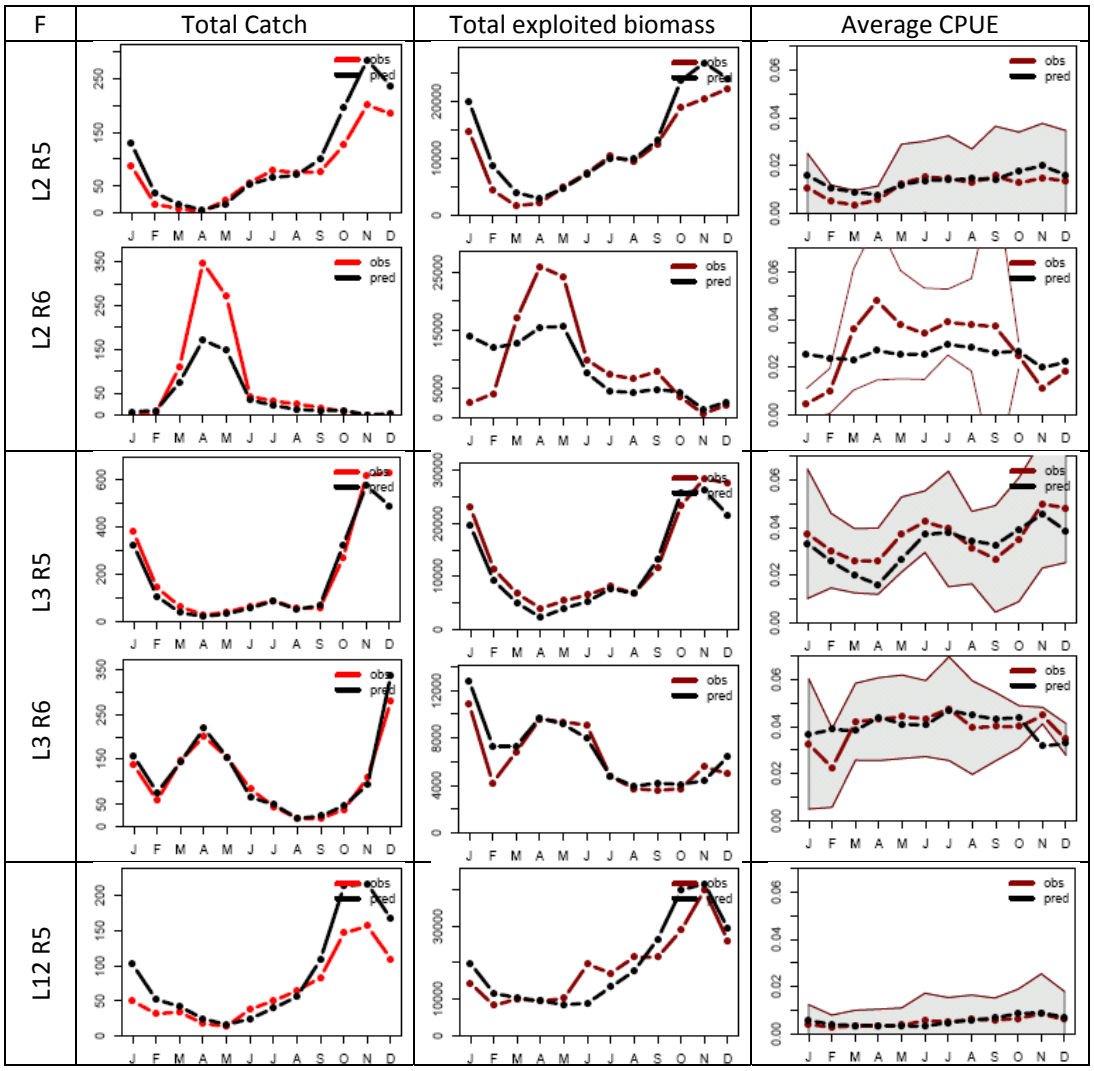

Figure 7.7: Monthly climatology of model predictions vs. observations in two EPO check zones (see map on Fig. 8.4). Shaded zone in average CPUE series corresponds to 95% CI.

Optimal Parameterization

This optimization experiment using the new fine age structure allowed estimating all key parameters of albacore, including the new larvae predator function parameter, which limits spatial boundaries of spawning ground by the critical values of MTL biomass (parameter α in Table 7.2).

Table 7.2: Estimates of habitats and movement parameters for south Pacific albacore using environmental forcings from NCEP-ORCA2

Parameters estimated by the model			**Unit**	**SODA 1° v1**	**SODA 1° v2**
T_s	Spawning	Optimum of the spawning temperature function	°C	[24.5	[24.5
σ_s		Std. Err. of the spawning temperature function	°C	2.5]	2.5*
α		Larvae food-predator trade-off coefficient	-	[3	4.98
T_a	Feeding habitat	Optimum of the adult temperature function at maximum age	°C	7.9	7.88
σ_a		Std. Err. of the adult temperature function at maximum age	°C	4]	5]
$\hat{O}$		Oxygen threshold value at Ψ_O =0.5	mL · L^{-1}	4.31	4.36
D_{max}	Move-ment	Diffusion parameter		0.10*	0.075*
V_{max}		Maximum sustainable speed	B.L. s^{-1}	1.8	1.8

*Fixed; [val = value close to minimum boundary value; val] = value close to maximum boundary value

Natural mortality

In the last stock assessment with MULTIFAN-CL (Hoyle et al 2012) the natural mortality was fixed to 0.4 yr-^{1} (0.033 mo^{-1}). For this revised experiment with SEAPODYM and NCEP configuration the mortality rate was estimated around 0.18 mo^{-1} for the larvae cohort decreasing rapidly to a value below 0.04 mo^{-1} (O.48 yr^{-1}) for the cohorts with age between 30 and 60 months (63-87 cm in size), then increasing again for the remaining oldest cohorts attaining the maximum value 0.08 mo^{-1} (Figure 7.8). Thus, the mortality rates estimated for the young fraction of the exploited stock is close to those used for the stock assessment with MULTIFAN-CL while adult mortality rates are estimated to be 50-100% higher.

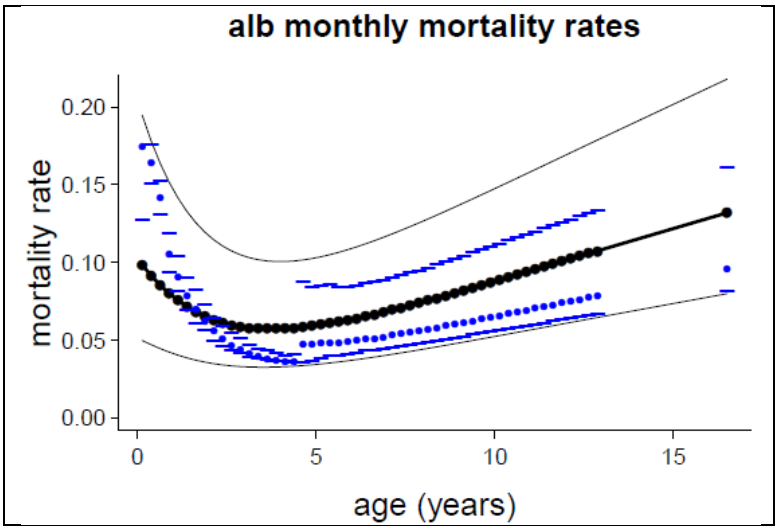

Figure 7.8: Natural mortality rates (month^{-1}) estimated from SEAPODYM optimization experiment.

Spawning and juvenile recruitment

Both parameters defining the spawning temperature function were estimated. The optimal temperature value slightly higher 24°C and standard error being 0.6 lead to a distribution of larvae concentrated between 24 and 27°C. A substantial progress was achieved with the estimate of the parameter α after separating the effects of predator and food in the spawning index. The model parameter α now controls the effect of predator density on the larvae habitat and thus their survival rate. It was also possible to estimate the seasonality of spawning migrations (), which resulted in the migration switch occurring two months earlier with respect to previous NCEP reference solution (switching feeding habitat to spawning in May and back to feeding in October).

Feeding habitat

The optimization approach suggests high sensitivity to dissolved oxygen concentration with a threshold value 2.6 ml$\cdot$ l^{-1}, which almost did not change from the previous NCEP experiment. The optimal temperature is estimated to range between 24.2°C (juveniles and spawners) and 6.2°C for the oldest/largest fish (Figure 7.9). The estimate for the optimal temperature for oldest cohort remains low; however after a closer look on the actual temperatures of the habitat, associated with biomass, one can see that modelled albacore occupy areas with temperatures between 16°C and 9°C at ages 4-200 months respectively and around 24°C at early stage (Figure 7.10). These values are consistent with previous description from fishing data occurrence (Sund et al 1981) and more recent results from individual tracking (Domokos et al. 2007).

Movements

The parameter controlling directed movements (advection) was estimated with a value V_{max} = 1.0 BL s^{-1}, which is relatively high compared to other species (e.g. V_{max} = 0.75 for skipjack). This result seems coherent given that this species has the most marked seasonal migration between feeding grounds in the subtropical convergence zone in the south and spawning ground in the sub-equatorial region.

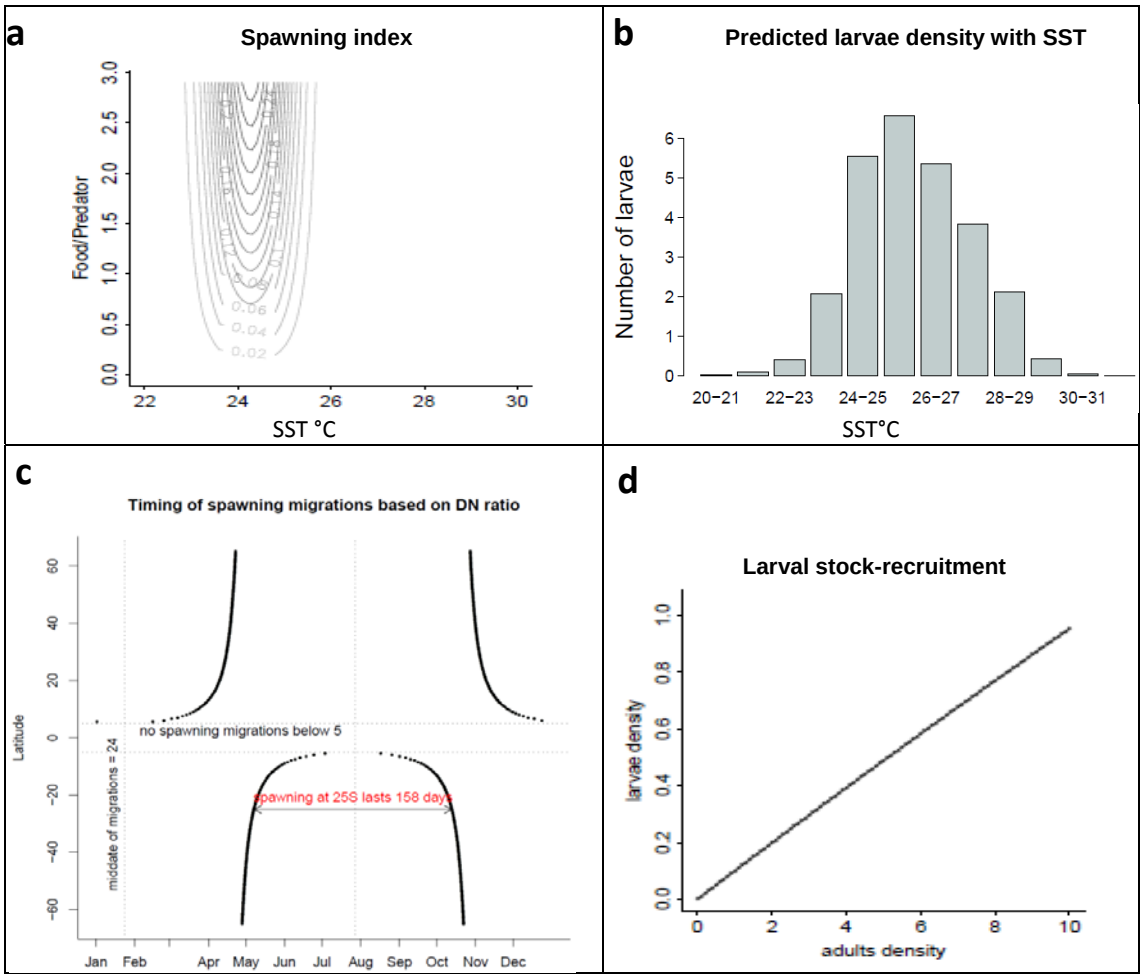

Figure 7.9: Spawning and larval recruitment. **a:** spawning index in relation to SST and food-predator tradeoff ratio. **b:** Distribution of larvae according to SST and the estimated parameters of spawning index.c: Seasonal timing of spawning migration. **d:** SEAPODYM larval stock-recruitment relationship estimated for albacore. Densities are in number of individual per km^2 for adult and 1000's of individual per km^2 for larvae.

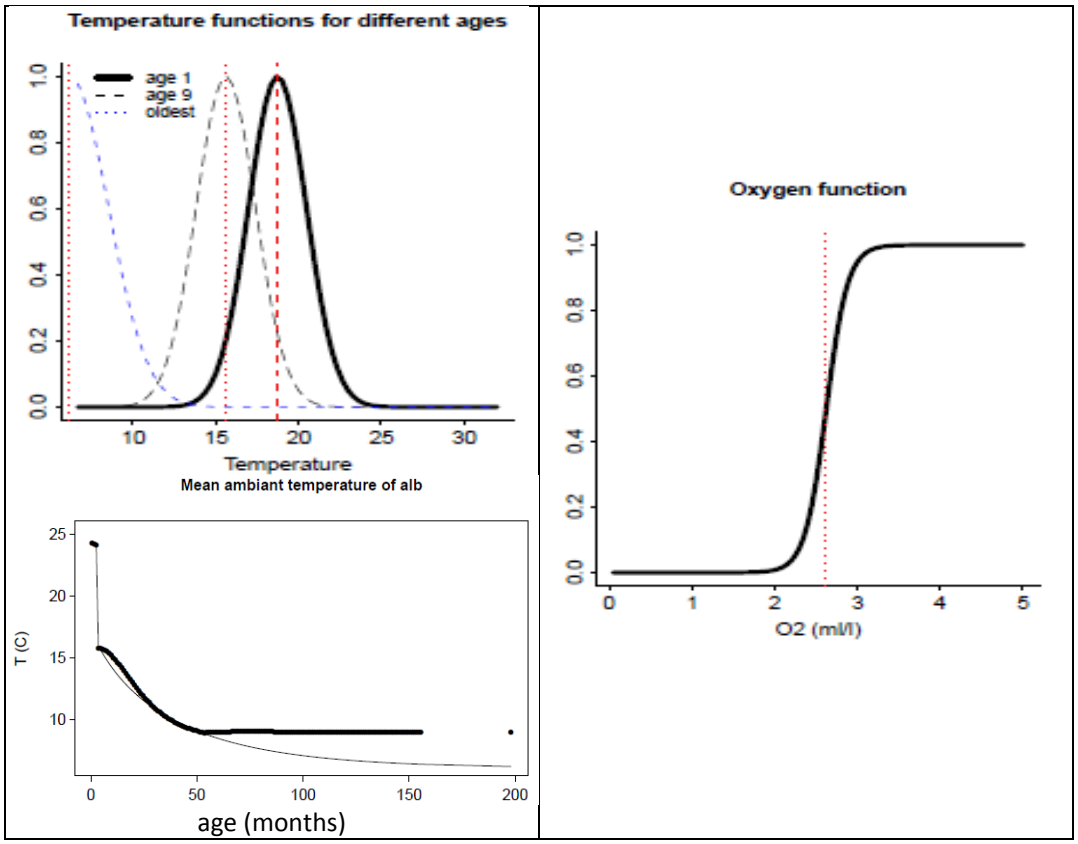

Figure 7.10: Optimized functions for temperature and oxygen habitats.

Biomass estimates and population dynamics

In the previous optimization experiments (both NCEP **2°** and SODA **1°** based) without the estimation of seasonality parameters and using an age structure discretization inconsistent with the model time step, the total biomass estimate with SEAPODYM was much higher than the MULTIFAN-CL estimate conducted in 2008 and 2012 (Hoyle et al 2008; Hoyle et al., 2012). Then, initial conditions of these first two SEAPODYM optimization experiments were forced to be close to those of MULTIFAN-CL. As a result both model estimates had similar biomass levels and temporal trends.

In this new experiment, the (unconstrained) total biomass estimate from SEAPODYM has decreased to ~1 million t, while in the same time the revised assessment with MULTIFAN-CL (Hoyle et al 2012) has more than doubled with an average value of ~1.4 million t between 2000-2007 (Figure 7.11). Therefore, the two most recent estimates form MULTIFAN-CL and SEAPODYM are converging.

Average seasonal variability

The mean spatial distributions (Figure 7.12 and Figure 7.13) show a clear distinction between life stages. Young immature albacore are predicted to concentrate in the western half part of the south Pacific basin between 20°S and 40°S with a decreasing eastward gradient of density, and without any apparent seasonal change in this pattern despite of the observed variability of catch, likely linked to ocean conditions. Conversely, adult fish show a clear north-south seasonal migration pattern. The density of adult is maximum in the latitudinal band 10°S-25°S during the 4th and still high during the

1st quarter and below 20°S or in the central Pacific between 10-20°S during the second quarter. Thus, the adult fish tend to concentrate seasonally in warm waters of the southern tropical area in austral summer for spawning and then move for feeding either south or toward the central sub-equatorial region.

Though the model predicts continuous spawning over the year opportunistically according to the environmental conditions, there is a strong seasonal peak in spring- summer coinciding with the maximum concentration of adult in the latitudinal band 10°S - 25°S. This is consistent with the result observed by Farley et al. (2013) in their stock-wide examination of the reproductive biology of south Pacific albacore.

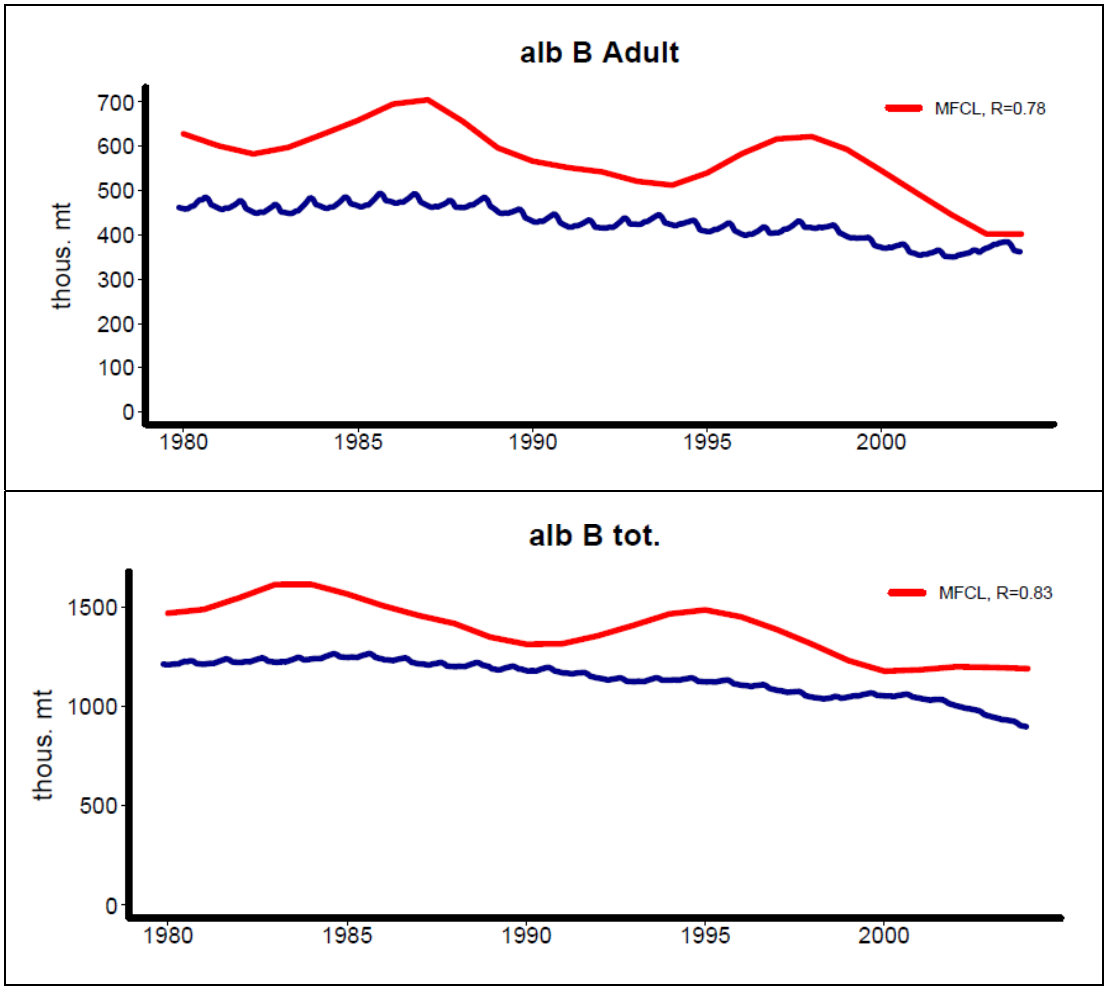

Figure 7.11: Estimates of total biomass of south Pacific albacore: top) estimates of total spawning biomass given by SEAPODYM (dark blue) and MULTIFAN-CL in 2012 (red) (Hoyle et al 2012); bottom) the same comparison but for the total albacore biomass (young + adult).

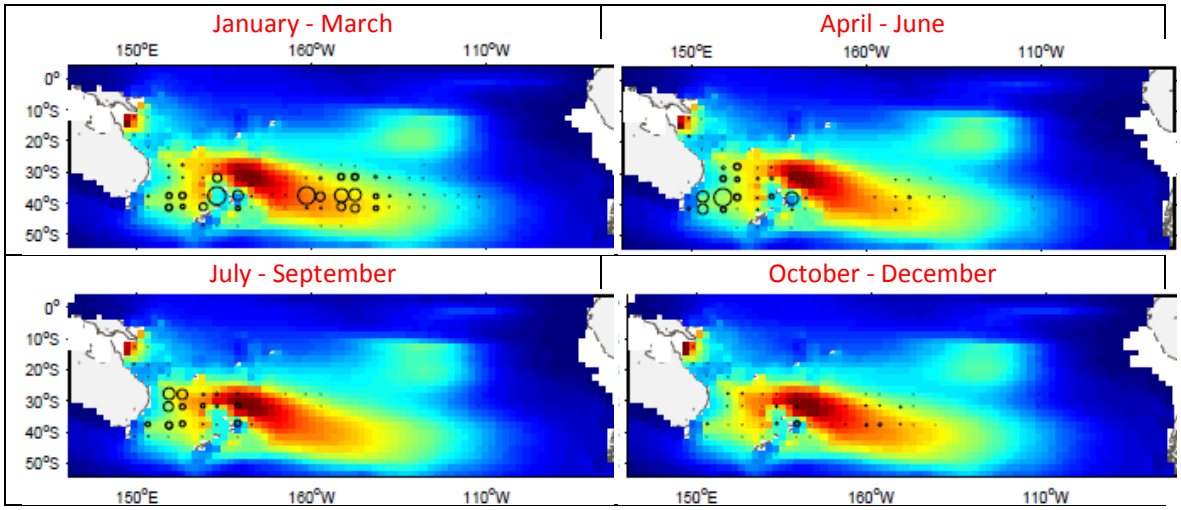

Figure 7.12 Seasonal spatial distributions of young (immature) albacore. Temporal average over 1990-1999.

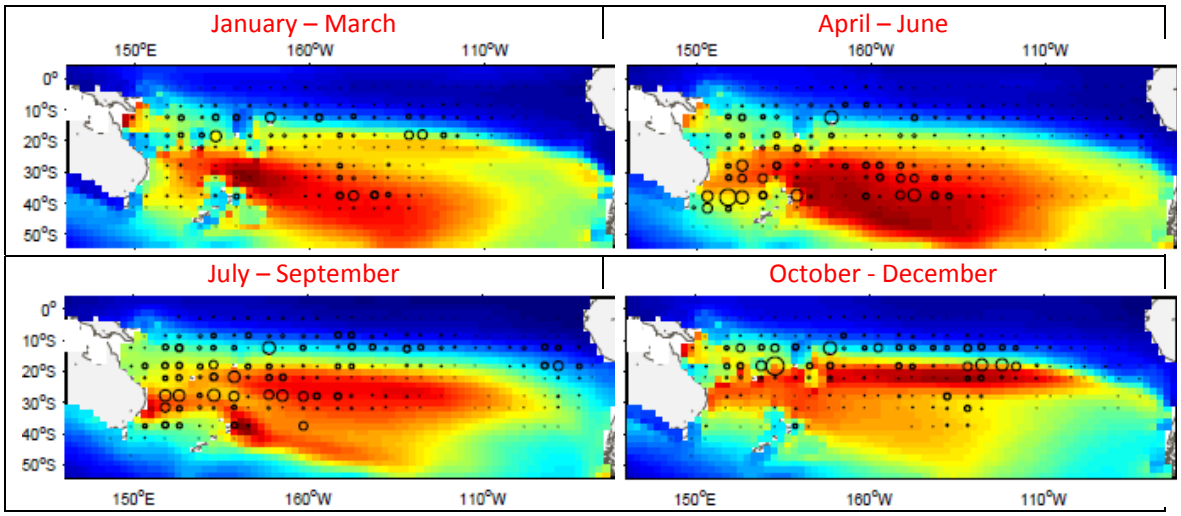

Figure 7.13: Seasonal spatial distributions of adult (mature) albacore. Temporal average over 1990-1999.

8. REFERENCE FIT FOR PACIFIC SKIPJACK FOR CLIMATE CHANGE ANALYSES

No change to the reference fit presented to 2011 WCPFC Scientific Committee meeting (SC7).

9. REFERENCE FIT FOR PACIFIC BIGEYE FOR CLIMATE CHANGE ANALYSES

Physical forcing: IPSL CM4

The IPSL-PISCES Earth Climate simulation provided physical-biogeochemical fields used to drive SEAPODYM and to investigate the responses of tuna population dynamics to global warming. The IPSL climate model (Marti et al., 2006) is composed of an oceanic physical component OPA, a sea ice component LIM, an atmospheric component LMDZ, and a land surface component ORCHIDEE, coupled through the OASIS coupler. The global climate simulation starts with climatological conditions and the only variable forcing is the change in atmospheric CO_2 concentration. The simulation uses the historical atmospheric CO_2 concentration between 1860 and 2000, which then increases according to the SRES A2 IPCC scenario for the 21st century, i.e., atmospheric CO_2 concentrations reaching 850 ppm in the year 2100. Physical forcing fields from the climate simulation have then been used to force an offline version of the oceanic biogeochemical model PISCES (Aumont and Bopp, 2006) over a similar period (1860-2100) and for the global ocean. A detailed description and evaluation of those simulations is provided in Sarmiento et al. (2004), and Schneider et al. (2007). The latitudinal anomaly in temperature was corrected as per the methods reported to SC7 and published in Lehodey et al. (2013).

Fishing data

The fishing data used was the same as the reference fit for the historical period.

Population structure

The population structure used was the same as the reference fit for the historical period.

Fit to catch data

The optimization experiment using corrected IPSL-CM4 temperature fields provided reasonable fit to fishing data for the historical period used (1982-2000) with good estimation of size frequency distribution by fishery. Relative error in catch was high only in regions with very low level of catch with an interesting exception along the latitudinal band 10°N-15°N in the WCPO (Figure 8.1).

Optimal Parameterization

The optimization was not able to correctly estimate some of parameters for habitat and movements (Table 8.1). The standard error of the spawning temperature function and the diffusion parameter

were fixed. The Optimum of the spawning temperature function and the standard error of the adult temperature function at maximum age were estimated near their lower and upper boundaries respectively.

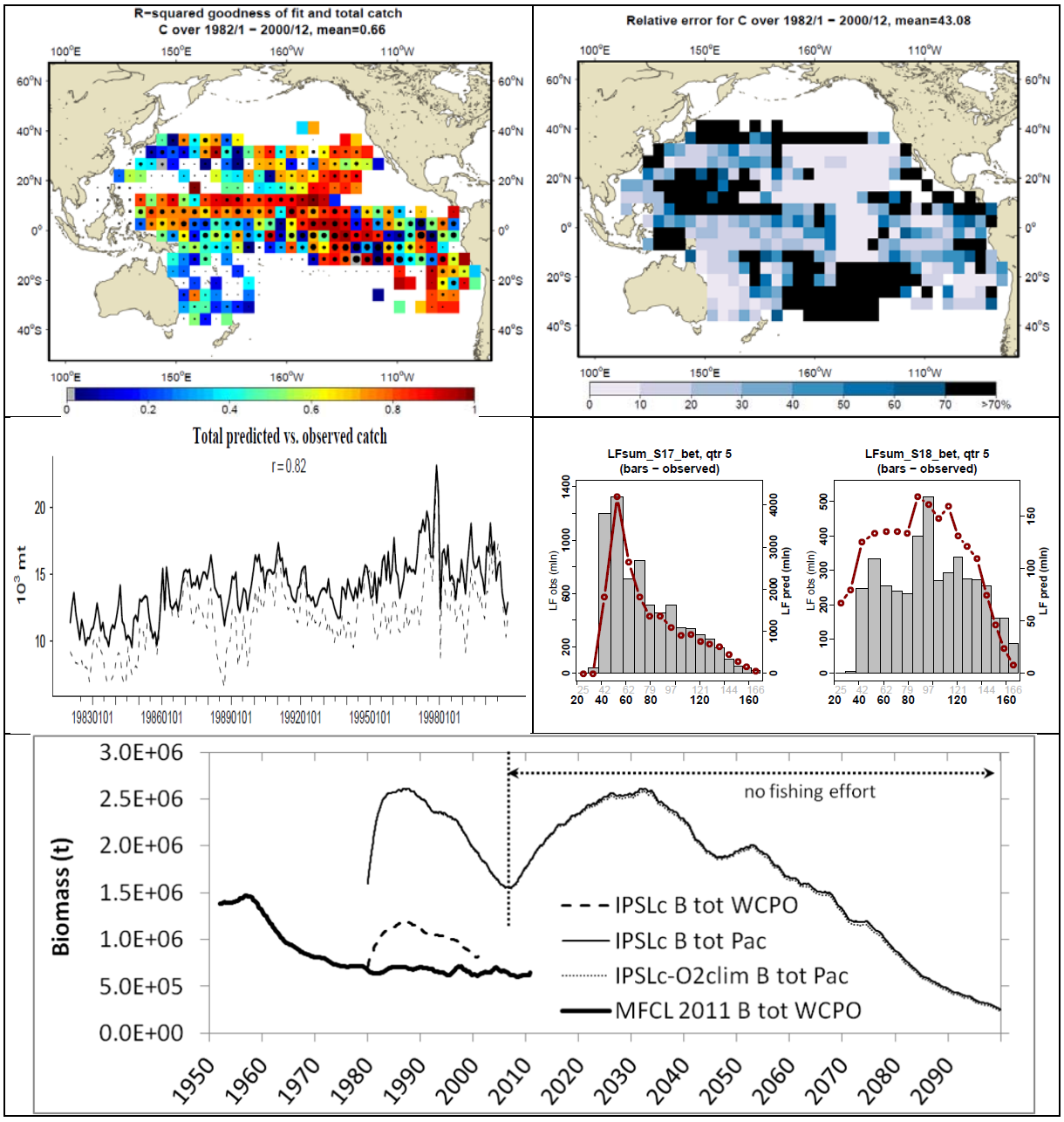

Figure 9.1: Bigeye optimization with IPSL-CM4 corrected forcing. From top to bottom and left to right: spatial correlation between predicted and observed catch over all the period 1982-2000 with black circles proportional to the level of catch; relative error in predicted catch for all fisheries over all the period 1982-2000; total predicted and observed catch; examples of fit between observed (histogram) and predicted size frequency of catch for two of the 17 fisheries used for optimization; total bigeye biomass estimates for the whole Pacific ocean and compared to the last WCPFC stock assessment estimate (MFCL 2011) in the WCPO (sum of regions 1 to 6 in Hoyle et al. 2011).

The estimates of parameter values indicates that the movement parameter is very low (< 0.2 body length s^{-1}), the standard error of spawning temperature (σ_s) function is narrow (0.75°C) while the larvae prey-predator tradeoff coefficient (α) is high (4.7). Usually, there is a correlation between σ_s and α; when one is increasing the other decreases, compensating their effect upon each other to some degree. To obtain convergence σ_s was fixed to a low value resulting in a high value of α. This means that spawning grounds were defined by concentrated, highly favourable areas and periods. A consequence of this parameterisation was a declining population contracting around its predicted core habitat where both spawning and feeding conditions need to exist together since mature fish were estimated to have small displacement capacity. Since tagging data analyses suggest that bigeye tuna can migrate long distances, this scenario seems highly less plausible, and optimization experiments including sensitivity analyses for these parameters need to be continued, in particular to investigate where are the bifurcation points from which opposite trends can emerge.

Table 8.1. Summary of parameters values estimated by optimization approach with IPSL forcing before (IPSL) and after correction (IPSLc) of bias in temperature fields. Colors give an indication of confidence (green = good; orange = low confidence; red = large uncertainty).

Parameters estimated by the model			Unit	**BET**	
				IPSL	IPSLc
		Habitats			
1	T_s	Optimum of the spawning temperature function	°C	26.2	28.4
2	σ_s	Std. Err. of the spawning temperature function	°C	0.9	0.75*
3	α	Larvae food-predator trade-off coefficient	-	0.34	4.7
4	T_a	Optimum of the adult temperature function at maximum age	°C	[8	10.6
5	σ_a	Std. Err. of the adult temperature function at maximum age	°C	5]	4.45
6	Ô	Oxygen threshold	$ml \cdot l^{-1}$	1.02	1.23
		Movements			
8	V_M	Maximum sustainable speed	$B.L.\cdot s^{-1}$	0.1	0.19

* fixed; [ ] reaching min or max value boundary

Biomass estimates and population dynamics

The total bigeye stock biomass in the WCPO (west of 150°W) was slightly over the estimate with the stock assessment model MFCL (Figure 8.1) but the decreasing trend in SEAPODYM was stronger. Biomass estimate at Pacific basin scale was more than the double with the decline in biomass since 1990 stronger than that observed for the WCPO. Fishing effort information was unavailable from 2008 for the simulation and the future projections are made in the absence of fishing mortality. The simulation suggests that at least two decades are required for the stock to rebuild and reach a new equilibrium.

The optimization with the corrected IPSL-CM4 forcing led to a continuous decline under the A2 scenario, even in the eastern Pacific, and the population finally collapses by the end of the Century. A second simulation using climatological fields of oxygen did not modify this result (Figure 8.1),

providing verification that this trend is not due to the predicted change for this variable. The validity of this simulation result however should be interpreted with caution as model exploration indicates some inconsistencies.

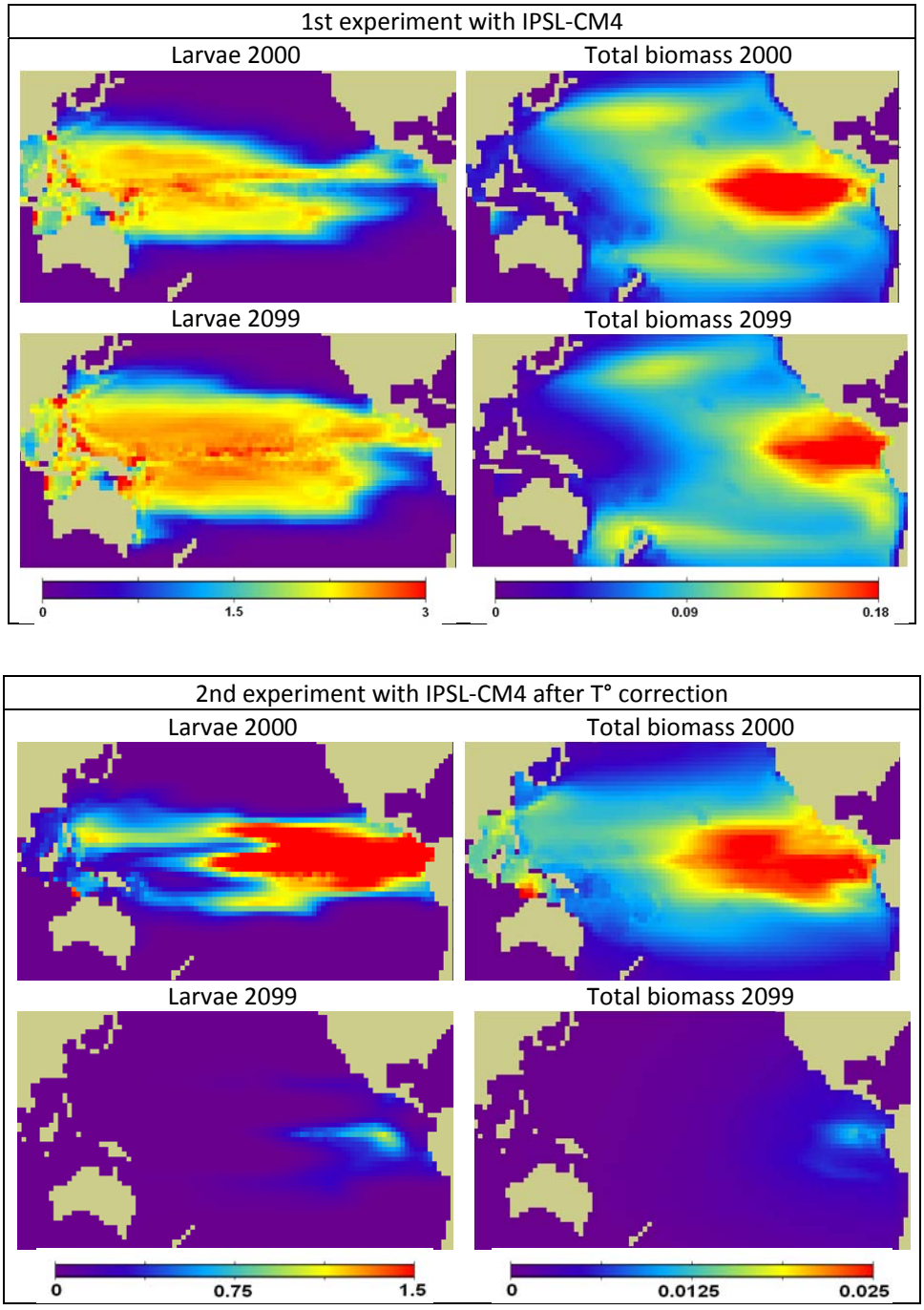

Figure 9.2: Mean annual density of bigeye larvae (ind. km^{-2}) and total biomass (t km^{-2}) predicted from the A2 climate scenario in 2000 and 2099 before and after temperature correction and new optimization experiment.

10. REFERENCE FIT FOR SOUTH PACIFIC ALBACORE FOR CLIMATE CHANGE ANALYSES

No change to the reference fit presented to 2012 WCPFC Scientific Committee meeting (SC8).

11. CURRENT AND FUTURE WORK PLAN

Swordfish

The first application of SEAPODYM to swordfish was presented to SC8. Development of a second generation model will commence in December 2013 for this species which will incorporate updated fisheries data provided to the WCPFC for this species.

Operational Basin scale model

A pre-operational model configuration of SEAPODYM has been developed for the Pacific skipjack population at weekly ¼° resolution, based on optimization achieved with SODA configuration (Lehodey et al. WCPFC 8). The environmental variables are provided by the ocean reanalysis GLORYSv2 and the Satellite derived primary production for the historical period and the operational ocean circulation model PSY3 of Mercator-Ocean for real-time and forecast. The stratification of fisheries is the same as the reference optimisation experiment with SODA, but with a monthly average fishing effort based on the last 2 years. The high resolution simulation shows the same large basin-scale patterns as the lower resolution (Figure 11.1Figure 11.1) but with a detailed representation of mesoscale activity.

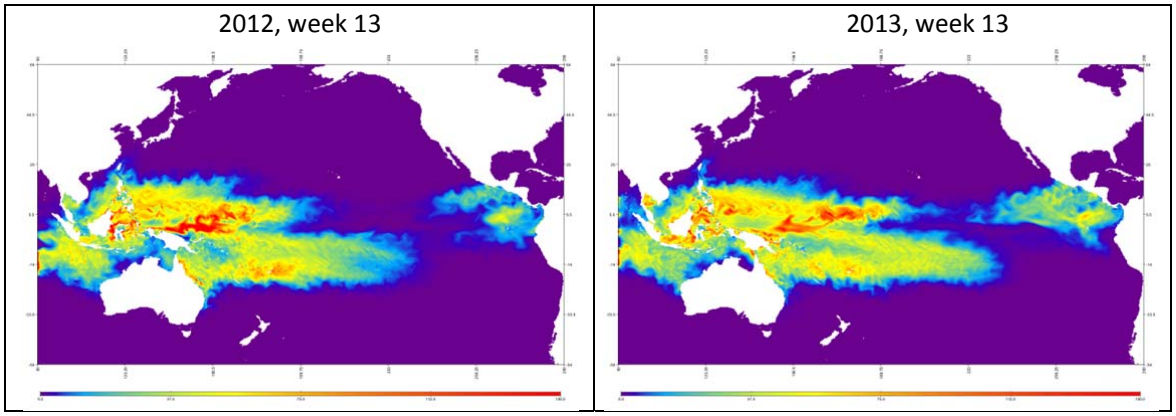

Figure 11.1. Pre-operational model at 0.25°x week. Distribution of larvae density predicted without fishing effort, for the calendar week 13 (March 25-31) in 2012 compared to 2013.

Sub-regional Modelling

There are technical challenges to implementing operational models at the sub-regional scale. First, tuna species are highly migratory species, and their habitats cover the whole ocean. Simulating the dynamics of these fish stocks at high resolution in a sub-region region requires accounting for the exchanges (fluxes) with the rest of the populations outside of the regional domain, under the influence of both environmental variability (e.g., El Niño events) and fishing mortality. Following the approach used in physical oceanography, the basin-scale SEAPODYM configuration at resolution of 1/4°x week can provide the open boundary conditions for a sub-regional model. This requires new technical developments in the code of the model to adapt its numerical scheme to the regionalisation.

A first application of this approach will be implemented for the EEZ of Indonesia. The sub-regional SEAPODYM operational model will be at resolution of 1/12°x day (Figure 11.2) and will use a climatological data set (i.e. monthly average) of fishing effort for the Indonesian waters prepared from the best available information to apply an average fishing mortality. This initiative should complements WCPFC efforts to improve the monitoring and management of tuna fisheries in this region that is of critical importance for the sustainability of tuna resources in the western and central Pacific Ocean generally. At the same time it will support the development of SEAPODYM operational model for skipjack yellowfin and bigeye tuna since these basin-scale configurations are necessary to provide boundary conditions for the regional Indonesian model configuration. The main objectives of this development are to:

- evaluate the operational model of tuna spatial dynamics (SEAPODYM) at a resolution of 1/12°x day for three species: skipjack, yellowfin and bigeye;
- promote the use of VMS data for estimating fishing effort and produce a database of operational fishing effort estimates that can be used both in the operational chain of modelling and to consolidate the national fishing statistics;
- provide capacity-building for a PhD Indonesian student working on Indonesian tuna fisheries and several engineers and technicians.
- demonstrate the interest of developing an Electronic catch Report System (ERS) that can be coupled to operational VMS and SEAPODYM to validate and monitor in real time the tuna stock and fisheries in the Indonesian EEZ.

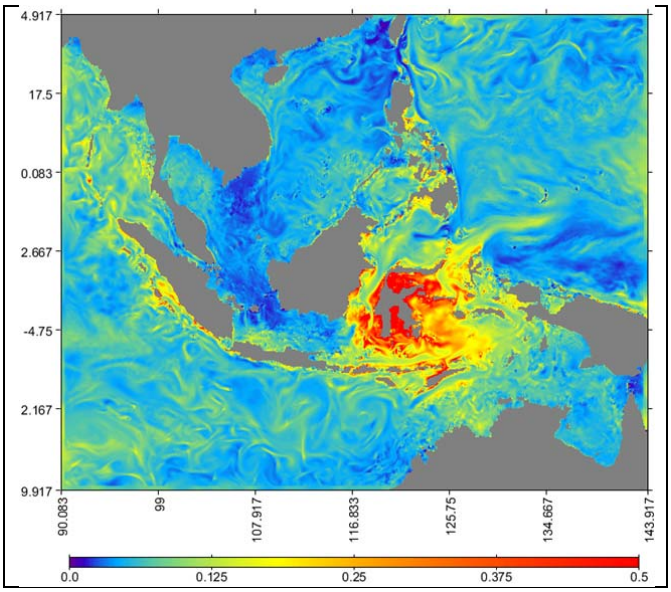

Figure 11.2. Domain of the regional operational model for the INDESO project illustrated with the 1st test for skipjack model.

Incorporation of tagging data

The incorporation of Pacific Ocean tagging data will commence once new physical forcing data (either SODA 1 degree and MERCATOR ¼ degree) are pre-processed for use in SEAPODYM. The revised SODA forcing should extend the modelling period to December 2009 and the MERCATOR forcing until December 2012. It is expected that new reference fits for each species will results through the applications of these new data sources (forcing and tagging).

Yellowfin Tuna

The development of the model for yellowfin tuna will commence in the later 2013 with the incorporation of tagging and new physical forcing data. The SC is expected to review at reference fit for this model at SC10.

Climate Change Modelling

The current physical forcing for the evaluation of climate change scenarios is restricted to a single CMIP4 model (IPSL). To capture the uncertainty in climate change projections an ensemble of CMIP5 models is under development. For the historical period a revised physical forcing that has realistic simulation of oceanic conditions, under the influence of ENSO and PDO variability, has been generated. The coupled NEMO-PISCES model has been forced by observed winds of the ERA-Interim reanalysis using the latest version (IFS5) covering the period 1979-present. Five to six CMIP5 models will be coupled with the NEMO-PISCES model to generate physical forcings under climate change. The choice of CMIP5 models has been determined by their compatibility with the historical forcing (so the jump from the historical forcing to the climate anomaly is minimised) and that they have realistic ENSO and PDO variability. This approach means that SEAPODYM only needs to be optimised

once for each species before simulation of various climate change scenarios can be implemented. A first version of these climate change simulations are expected to be presented to SC10.

SEAPODYMview

The software SEAPODYMview which provides for easy display of SEAPODYM output is currently being revised to allow use on non-Linux operating systems and to provide improved visualisation options.

12. REFERENCES

Bell JD, Ganachaud A., Gehrke PC, Griffiths SP, Hobday AJ, Hoegh-Guldberg O, Johnson, JE Le Borgne R, Lehodey P, Lough JM, Matear RJ, Pickering TD, Pratchett MS, Sen Gupta A, Senina I and Waycott M., (2013) Tropical Pacific fisheries and aquaculture will respond differently to climate change. *Nature Climate Change,* 3: 591-599

Farley, J.H., A.J. Williams, C.R. Davies, S.J. Nicol. 2013. Reproductive dynamics of South Pacific albacore tuna (Thunnus alalunga). Plos ONE, 8: e60577.

Lehodey P., Murtugudde R., Senina I. (2010). Bridging the gap from ocean models to population dynamics of large marine predators: a model of mid-trophic functional groups. *Progress in Oceanography*, **84**: 69–84

Lehodey P., Senina I., & Murtugudde R. (2008). A Spatial Ecosystem And Populations Dynamics Model (SEAPODYM) - Modelling of tuna and tuna-like populations. *Progress in Oceanography,* **78**: 304-318.

Lehodey P., Senina I., Calmettes B, Hampton J, Nicol S. (2013). Modelling the impact of climate change on Pacific skipjack tuna population and fisheries. *Climatic Change,* 119: 95–109.

Lehodey P., Senina I., Calmettes B., Hampton J., Nicol S., Williams P., Jurado Molina J., Ogura M., Kiyofuji H., Okamoto S. (2011). SEAPODYM working progress and applications to Pacific skipjack tuna population and fisheries. 7th regular session of the Scientific Steering Committee, 8-17 August 2011, Pohnpei, Federate States of Micronesia. WCPFC-SC7-2011/EB- WP 06.

Lehodey P., Senina I., Sibert J., Bopp L, Calmettes B., Hampton J., Murtugudde R. (2010). Preliminary forecasts of population trends for Pacific bigeye tuna under the A2 IPCC scenario. *Progress in Oceanography.* 86: 302–315

Lehodey, P., Hampton, J., Brill, R.W., Nicol, S., Senina, I., Calmettes, B., Pörtner, H.O., Bopp, L., Ilyina,T., Johann D. Bell, and J. Sibert (*in press*). Vulnerability of oceanic fisheries in the tropical Pacific to climate change. *In* Bell J., Johnson JE, Hobday AJ (Ed.), Vulnerability of Tropical Pacific Fisheries and Aquaculture to Climate Change. Secretariat of the Pacific Community. Noumea New Caledonia.

Lehodey, P., Senina, I., Hampton, J, Nicol, S, Williams, P., Jurado Molina J., Abecassis, M., Polovina J. Project 62: SEAPODYM working progress and applications to Pacific tuna and billfish populations and fisheries. 8th regular session of the Scientific Steering Committee, 7-15 August 2012, Busan, Korea. WCPFC-SC8-2012/EB-IP-06.

Senina I, Royer F, Lehodey P, Hampton J, Nicol S, Ogura M, Kiyofuji H, Sibert J (2012). Integrating conventional and electronic tagging data into SEAPODYM. Pelagic Fisheries Research Program, Newsletter 16(1): 9-14

Senina I., Sibert J., & Lehodey P. (2008). Parameter estimation for basin-scale ecosystem-linked population models of large pelagic predators: application to skipjack tuna. *Progress in Oceanography*, **78**: 319-335.

Sibert J, Senina I, Lehodey P, Hampton J. (2012). Shifting from marine reserves to maritime zoning for conservation of Pacific bigeye tuna (*Thunnus obesus*). *Proceedings of the National Academy of Sciences* 109(44): 18221-18225.